AD_____

Award Number: DAMD17-99-1-9031

TITLE: Pericellular Hyaluronan and Prostate Cancer

PRINCIPAL INVESTIGATOR: Charles B. Underhill, Ph.D.

CONTRACTING ORGANIZATION: Georgetown University Medical Center
Washington, DC 20007

REPORT DATE: July 2002

TYPE OF REPORT: Final

PREPARED FOR: U.S. Army Medical Research and Materiel Command
Fort Detrick, Maryland 21702-5012

DISTRIBUTION STATEMENT: Approved for Public Release;
Distribution Unlimited

The views, opinions and/or findings contained in this report are
those of the author(s) and should not be construed as an official
Department of the Army position, policy or decision unless so
designated by other documentation.

REPORT DOCUMENTATION PAGE			Form Approved OMB No. 074-0188

Public reporting burden for this collection of information is estimated to average 1 hour per response, including the time for reviewing instructions, searching existing data sources, gathering and maintaining the data needed, and completing and reviewing this collection of information. Send comments regarding this burden estimate or any other aspect of this collection of information, including suggestions for reducing this burden to Washington Headquarters Services, Directorate for Information Operations and Reports, 1215 Jefferson Davis Highway, Suite 1204, Arlington, VA 22202-4302, and to the Office of Management and Budget, Paperwork Reduction Project (0704-0188), Washington, DC 20503

1. AGENCY USE ONLY (Leave blank)	2. REPORT DATE July 2002	3. REPORT TYPE AND DATES COVERED Final (1 Jan 99 -30 Jun 02)	

4. TITLE AND SUBTITLE Pericellular Hyaluronan and Prostate Cancer	5. FUNDING NUMBERS DAMD17-99-1-9031

6. AUTHOR(S):
Charles B. Underhill, Ph.D.

7. PERFORMING ORGANIZATION NAME(S) AND ADDRESS(ES) Georgetown University Medical Center Washington, DC 20007 E-Mail: underhic@georgetown.edu	8. PERFORMING ORGANIZATION REPORT NUMBER

9. SPONSORING / MONITORING AGENCY NAME(S) AND ADDRESS(ES) U.S. Army Medical Research and Materiel Command Fort Detrick, Maryland 21702-5012	10. SPONSORING / MONITORING AGENCY REPORT NUMBER

11. SUPPLEMENTARY NOTES
Original contains color plates: All DTIC reproductions will be in black and white.

12a. DISTRIBUTION / AVAILABILITY STATEMENT Approved for Public Release; Distribution Unlimited	12b. DISTRIBUTION CODE

13. Abstract *(Maximum 200 Words)* *(abstract should contain no proprietary or confidential information)*

The working hypothesis of the present project is that hyaluronan (HA) promotes tumor growth by maintaining pericellular spaces that allows the diffusion of nutrients. To test this hypothesis, we have carried out the following three tasks. First, the cDNA for human HA synthase (HAS3) was cloned and transfected into TSU causing them to over-express HA. The resulting cells grew faster than the control cells. In addition, histological examination of the tumors indicated that the HAS3 transfectants had increased intercellular space rich in HA and had greater number of blood vessels. Secondly, TSU cells were transfected with anti-sense vectors to HAS3, which caused them to express reduced levels of HA. These cells were found to grow slower than their control transfected counter-parts. And thirdly, we examined the effects of hyaluronidase on the growth of tumor xenografts on the chorioallantoic membranes of chicken embryos. Contrary to our expectations, hyaluronidase caused an increase in the size of the xenografts due in part to the induction of hemorrhages. This suggests that HA plays a role in maintaining the structural integrity of the blood vessels. Collectively, these results support our working hypothesis that HA promotes tumor progression.

14. SUBJECT TERMS prostate, hyaluronan, extracellular matrix, hyaluronan synthase, angiogenesis			15. NUMBER OF PAGES 32
			16. PRICE CODE

17. SECURITY CLASSIFICATION OF REPORT Unclassified	18. SECURITY CLASSIFICATION OF THIS PAGE Unclassified	19. SECURITY CLASSIFICATION OF ABSTRACT Unclassified	20. LIMITATION OF ABSTRACT Unlimited

NSN 7540-01-280-5500

Standard Form 298 (Rev. 2-89)
Prescribed by ANSI Std. Z39-18
298-102

Table of Contents

INTRODUCTION:

The present application is concerned with the role of hyaluronan (HA) in the progression of prostate cancer. HA is a large, negatively-charged carbohydrate that is found in many extracellular matricies. In our working hypothesis, we have proposed that HA is responsible for maintaining pericellular spaces between the nests of prostate tumor cells that is vital for the diffusion of nutrients. Without this pericellular space, tumor cells located only a short distance away from the blood supply will not receive an adequate supply of nutrients and will undergo necrosis. To test this working hypothesis, we have proposed the following specific aims:

1. We will examine the effects of increased HA production on tumor growth. For this we will transfect TSU cells (derived from human prostate cancer) with an expression vector for HA synthase, and the transfected clones as well as controls will be injected into nude mice. If our hypothesis is correct, then clones transfected with HA synthase will grow in the nude mice, while the control clones will not.

2. We will examine the effects of down regulating the synthesis of HA on the growth of prostate tumor cells. For this, we will examine the human prostate cell line TSU that produce large amounts of HA and readily grow in nude mice. These cells will be transfected with an antisense vector for HA synthase and then injected into nude mice along with control clones. If our hypothesis is correct then the transfected cells will grow at a slower rate and have less vascularization than the control cells. The transfected clones as well as control clones will be injected into nude mice. If our hypothesis is correct, then the hyaluronidase transfected cells should have a reduced growth rate as compared to control cells.

3. We will examine the effects of removing pericellular HA with hyaluronidase. In our revised approach, tumor cells will be grown on the chorioallantoic membranes of chicken embryos and hyaluronidase will be injected into some of the embryos. Again, if our hypothesis is correct then the tumors treated with hyaluronidase should grow at a slower rate than the control tumors.

BODY

Hyaluronan (HA) is a large, negatively-charged carbohydrate that is present in many extracellular matrices. A number of previous studies have suggested that the production of hyaluronan (HA) is associated with the metastatic behavior of tumor cells (1-11). Based on this and a variety of other evidence, we have proposed that pericellular HA can enhance tumor cell growth by maintaining channels in the extracellular matrix, through which nutrients can diffuse. To test this possibility, we have proposed to manipulate the production of HA by tumor cells and examine the effect on their behavior.

We have completed work on all 3 tasks. Task 1 involves the transfection of tumor cells with expression vectors for HAS3, one of the enzymes that is responsible for the synthesis of HA (12-19). We have accomplished most of the original goals of task 1 which have been published by *Cancer Research* (see appendix). Task 2 consists of the down regulation of HA synthesis by transfection of tumor cells with anti-sense vectors to HAS. We have also completed most of these goals and are presently preparing a manuscript describing the results of this study. Task 3 consists of examining the effect of hyaluronidase on the growth of tumor cells on the chorioallantoic membrane of chicken embryos. Contrary to our expectations, the treatment with hyaluronidase increase the size of the tumor rather than reducing it. However, further examination revealed that this increase in size was due to the formation of hemorrhages in the tumor xenografts. Thus, our original hypothesis that HA promotes tumor cell growth is still valid. These results have been submitted for publication.

TASK 1. The Effects of Increased HA Expression on Tumor Growth: As indicated above, the goals of this task have for the most part been completed and the results have been published in *Cancer Research* (see appendix). The results being reported in this section are essentially identical to that in the published manuscript and what was reported in the previous the previous progress reports.

To test our working hypothesis that HA promotes the growth of tumor cells, we have transfected a human prostate cancer cell line with an expression vector for HA synthase. Initially, we had proposed to the LNCaP cell line, however in preliminary studies we found that these cells do not readily grow in CAM of chicken embryos or in nude mice. For this reason, we have switched to the TSU cell line that readily grows in these two model systems. These cells were transfected with expression vectors containing candies for mammalian HA synthase 3 that we isolated from a library of human brain cDNA.

1.1. Isolation of cDNA for HAS-3: The full length cDNA for HAS3 was cloned from a cDNA library of human brain using a probe consisting of the partial sequence of the gene. The open reading frame contained 1,659 base pairs corresponding to 553 amino acids as shown in Fig. 1. The HAS3 protein has a deduced molecular weight about 63 kDa and an isoelectric point of 8.70. The first 27 amino acid correspond to the signal peptide and there are six potential transmembrane domains. Between the first (amino acid 43 to 65) and second transmembrane domains (amino acid 384 to 402), there is a stretch of 317 amino acids, which may be the major functional region for polysaccharide synthase. The remaining 170 amino acids in the C terminal region (from amino acid 403 to 553) contain 4 transmembrane domains that can form two loops spanned in and out of membrane. There is a potential site for N-glycosylation site on amino acid 462, a glycosaminoglycan attachment site on position 464, and several phosphorylation sites for tyrosine kinase, casein kinase, protein kinase C and cAMP-and cGMP-dependent protein kinase. Comparison with related enzymes indicates that human HAS3 has about 53% identity to HAS1 (both human and mouse form), 67% identity to HAS2 and 96% identity to mouse HAS3. HAS3 also contains seven HA-binding motifs of $B(X_7)B$ in which B is either R or K and X_7

```
  1 ATG CCG GTG CAG CTG ACG ACA GCC CTG CGT GTG GTG GGC ACC AGC CTG TTT GCC CTG GCA  60
  1  M   P   V   Q   L   T   T   A   L   R   V   V   G   T   S   L   F   A   L   A   20

 61 GTG CTG GGT GGC ATC CTG GCA GCC TAT GTG ACG GGC TAC CAG TTC ATC CAC ACG GAA AAG 120
 21  V   L   G   G   I   L   A   A   Y   V   T   G   Y   Q   F   I   H   T   E   K   40

121 CAC TAC CTG TCC TTC GGC CTG TAC GGC GCC ATC CTG GGC CTG CAC CTG CTC ATT CAG AGC 180
 41  H   Y   L   S   F   G   L   Y   G   A   I   L   G   L   H   L   L   I   Q   S   60

181 CTT TTT GCC TTC CTG GAG CAC CGG CGC ATG CAA CGT GCC GGC CAG GCC CTG AAG CTG CCC 240
 61  L   F   A   F   L   E   H   R   R   M   Q   R   A   G   Q   A   L   K   L   P   80

241 TCC CCG CGG CGG GGC TCG GTG GCA CTG TGC ATT GCC GCA TAC CAG GAG GAC CCT GAC TAC 300
 81  S   P   R   R   G   S   V   A   L   C   I   A   A   Y   Q   E   D   P   D   Y  100

301 TTG CGC AAG TGC CTG CGC TCG GCC CAG CGC ATC TCC TTC CCT GAC CTC AAG GTG GTC ATG 360
101  L   R   K   C   L   R   S   A   Q   R   I   S   F   P   D   L   K   V   V   M  120

361 GTG GTG GAT GGC AAC CGC CAG GAG GAC GCC TAC ATG CTG GAC ATC TTC CAC GAG GTG CTG 420
121  V   V   D   G   N   R   Q   E   D   A   Y   M   L   D   I   F   H   E   V   L  140

421 GGC GGC ACC GAG CAG GCC GGC TTC TTT GTG TGG CGC AGC AAC TTC CAT GAG GCA GGC GAG 480
141  G   G   T   E   Q   A   G   F   F   V   W   R   S   N   F   H   E   A   G   E  160

481 GGT GAG ACG GAG GCC AGC CTG CAG GAG GGC ATG GAC CGT GTG CGG GAT GTG GTG CGG GCC 540
161  G   E   T   E   A   S   L   Q   E   G   M   D   R   V   R   D   V   V   R   A  180

541 AGC ACC TTC TCG TGC ATC ATG CAG AAG TGG GGA GGC AAG CGC GAG GTC ATG TAC ACG GCC 600
181  S   T   F   S   C   I   M   Q   K   W   G   G   K   R   E   V   M   Y   T   A  200

601 TTC AAG GCC CTC GGC GAT TCG GTG GAC TAC ATC CAG GTG TGC GAC TCT GAC ACT GTG CTG 660
201  F   K   A   L   G   D   S   V   D   Y   I   Q   V   C   D   S   D   T   V   L  220

661 GAT CCA GCC TGC ACC ATC GAG ATG CTT CGA GTC CTG GAG GAG GAT CCC CAA GTA GGG GGA 720
221  D   P   A   C   T   I   E   M   L   R   V   L   E   E   D   P   Q   V   G   G  240

721 GTC GGG GGA GAT GTC CAG ATC CTC AAC AAG TAC GAC TCA TGG ATT TCC TTC CTG AGC AGC 780
241  V   G   G   D   V   Q   I   L   N   K   Y   D   S   W   I   S   F   L   S   S  260

781 GTG CGG TAC TGG ATG GCC TTC AAC GTG GAG CGG GCC TGC CAG TCC TAC TTT GGC TGT GTG 840
261  V   R   Y   W   M   A   F   N   V   E   R   A   C   Q   S   Y   F   G   C   V  280

841 CAG TGT ATT AGT GGG CCC TTG GGC ATG TAC CGC AAC AGC CTC CTC CAG CAG TTC CTG GAG 900
281  Q   C   I   S   G   P   L   G   M   Y   R   N   S   L   L   Q   Q   F   L   E  300

901 GAC TGG TAC CAT CAG AAG TTC CTA GGC AGC AAG TGC AGC TTC GGG GAT GAC CGG CAC CTC 960
301  D   W   Y   H   Q   K   F   L   G   S   K   C   S   F   G   D   D   R   H   L  320

961 ACC AAC CGA GTC CTG AGC CTT GGC TAC CGA ACT AAG TAT ACC GCG CGC TCC AAG TGC CTC 1020
321  T   N   R   V   L   S   L   G   Y   R   T   K   Y   T   A   R   S   K   C   L  340

1021 ACA GAG ACC CCC ACT AAG TAC CTC CGG TGG CTC AAC CAG CAA ACC CGC TGG AGC AAG TCT 1080
341  T   E   T   P   T   K   Y   L   R   W   L   N   Q   Q   T   R   W   S   K   S  360

1081 TAC TTC CGG GAG TGG CTC TAC AAC TCT CTG TGG TTC CAT AAG CAC CAC CTC TGG ATG ACC 1140
361  Y   F   R   E   W   L   Y   N   S   L   W   F   H   K   H   H   L   W   M   T  380

1141 TAC GAG TCA GTG GTC ACG GGT TTC TTC CCC TTC TTC CTC ATT GCC ACG GTT ATA CAG CTT 1200
381  Y   E   S   V   V   T   G   F   F   P   F   F   L   I   A   T   V   I   Q   L  400

1201 TTC TAC CGG GGC CGC ATC TGG AAC ATT CTC CTC TTC CTG CTG ACG GTG CAG CTG GTG GGC 1260
401  F   Y   R   G   R   I   W   N   I   L   L   F   L   L   T   V   Q   L   V   G  420

1261 ATT ATC AAG GCC ACC TAC GCC TGC TTC CTT CGG GGC AAT GCA GAG ATG ATC TTC ATG TCC 1320
421  I   I   K   A   T   Y   A   C   F   L   R   G   N   A   E   M   I   F   M   S  440

1321 CTC TAC TCC CTC CTC TAT ATG TCC AGC CTT CTG CCG GCC AAG ATC TTT GCC ATT GCT ACC 1380
441  L   Y   S   L   L   Y   M   S   S   L   L   P   A   K   I   F   A   I   A   T  460

1381 ATC AAC AAA TCT GGC TGG GGC ACC TCT GGC CGA AAA ACC ATT GTG GTG AAC TTC ATT GGC 1440
461  I   N   K   S   G   W   G   T   S   G   R   K   T   I   V   V   N   F   I   G  480

1441 CTC ATT CCT GTG TCC ATC TGG GTG GCA GTT CTC CTG GGA GGG CTG GCC TAC ACA GCT TAT 1500
481  L   I   P   V   S   I   W   V   A   V   L   L   G   G   L   A   Y   T   A   Y  500

1501 TGC CAG GAC CTG TTC AGT GAG ACA GAG CTA GCC TTC CTT GTC TCT GGG GCT ATA CTG TAT 1560
501  C   Q   D   L   F   S   E   T   E   L   A   F   L   V   S   G   A   I   L   Y  520

1561 GGC TGC TAC TGG GTG GCC CTC CTC ATG CTA TAT CTG GCC ATC ATC GCC CGG CGA TGT GGG 1620
521  G   C   Y   W   V   A   L   L   M   L   Y   L   A   I   I   A   R   R   C   G  540

1621 AAG AAG CCG GAG CAG ACA AGC TTG GCT TTT GCT GAA GTG TGA 1662
541  K   K   P   E   Q   T   S   L   A   F   A   E   V   *  553
```

Fig. 1. Structural characteristics of human HAS3. The complete nucleotide sequence and the deduced amino acid sequences of human HAS3 are shown.
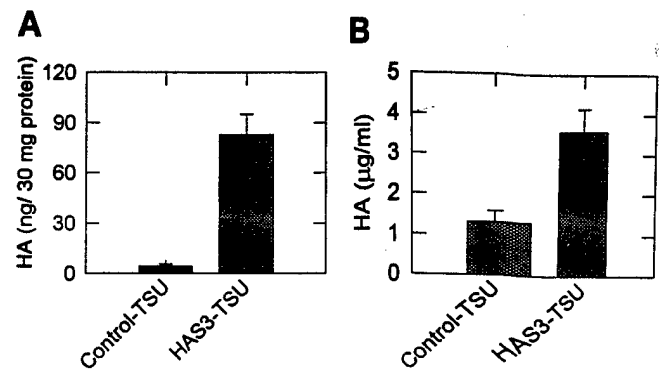

Fig. 2. Production of HA by vector control and HAS3 transfected TSU cells. Both control and HAS3 transfected cells were grown to confluence and then the cell layer and medium were analyzed for HA content using a modified enzyme linked assay. A. The amount of cell layer associated HA (normalized to the protein concentration) was higher in the HAS3TSU cells than in the control TSU cells. B. The amount of HA secreted into the medium by the HAS3-TSU cells was greater than that of the control-TSU cells. Note that most of the HA was secreted into the medium.
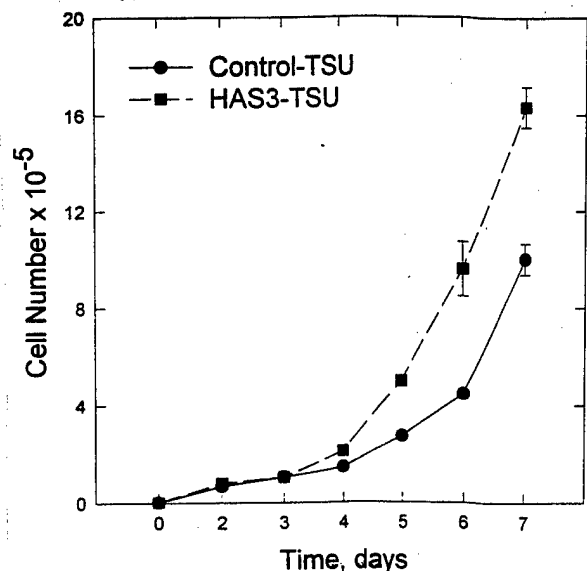

Fig. 3. The proliferation of control and HAS3 transfected TSU cells. The cell lines were cultured 24 well dishes in complete medium, that was changed ever other day. At the indicated time, a set of wells were harvested with a solution of EDTA in PBS and the cell numbers were determined with a Coulter counter. At low densities, no differences in the growth rates were apparent. However, at higher densities, the HAS3 transfected cells grew at a faster rate. Three replicates of this experiment gave similar results.

contains no acidic residues and at least one basic amino acid (25). Similar domains are present in other HA-binding proteins such as RHAMM, CD44, hyaluronidase, link protein, aggrecan, human GHAP and TSG-6. These results are consistent with earlier studies of this and related genes (13-19).

1.2. Expression of HA in TSU cells by transfection of human HAS3. To examine the role of HAS3 in tumor progression, the cloned cDNA was inserted into a mammalian expression vector (pcDNA3) under the control of a CMV promoter and transfected into TSU (human prostate cancer) cells. To avoid complications associated with clonal variations, all of the clones that survived in 1 mg/ml of G418 were pooled and expanded for experimental analysis throughout this study.

The production of HA by these cells was examined by a modified enzyme linked assay. As shown in Fig. 2, HAS3-TSU cells produced significantly greater amounts of medium and cell-associated HA than the control-TSU cells. These finding were confirmed by dot blotting of the conditioned medium onto nitrocellulose followed by peroxidase-linked HA staining (data not shown). It is important to note that the amount of secreted HA was significantly higher than that associated with the cell layer.

Cultures of the vector and HAS3 transfected TSU cells were then compared with respect to their HA staining pattern. At low densities, there was little obvious difference between the cell types, both of which expressed similar levels of HA that was present in the cytoplasm and on the cell surface (data not shown). Presumably this was due to the endogenous HA synthase present in the TSU cells that is active in the growing cells and masks the effect of the transfected HAS3. However, at high densities significant differences became apparent (Fig. 3). The control-TSU cells displayed a cobble-stone appearance indicative of contact inhibition of growth, and the production of HA was significantly down regulated (Fig. 3 A). In contrast, the HAS3-TSU cells appeared to have lost contact-inhibition of growth, forming numerous multi-layered clusters of cells, with which most of the HA staining was associated (Fig. 3 B). We believe that in these higher density cultures, the endogenous HA synthase is down-regulated due to contact inhibition of growth (26-29) and under these conditions the constitutive expression of the transfected HAS3 gene (controlled by the CMV promoter) becomes more prominent.

Taken together, the results of this section indicate that the transfection of HAS3 into TSU cells stimulates their expression of HA.

1.3. HAS3 Promotes Cell Growth at High Densities. We then compared the growth rates of the control and HAS3 transfected cells. For this, the cells were transferred to multi-well dishes, and at various times the cells were harvested and enumerated with a Coulter counter. Figure 4 shows that during the initial stages of the assay while the cells were still at low density, there was no obvious difference in the proliferation rates of the control and HAS3 transfected cells. However, beginning on day 4, when the cell densities were higher, the HAS3-TSU cells proliferated at a faster rate that the control cells. Similar results were obtained in three separate replications of this experiment. Thus, at high densities, the HAS3 transfected cells grow at a faster rate, presumably because they has lost part of their contact inhibition of growth and have the ability to form multi-layered clusters.

As indicated earlier, transfection of cells with HAS3 increase the levels of HA in both the medium and the cell-layer fractions, either of which could be responsible for the enhanced growth rate. To distinguish between these two fractions, we added varying concentrations of highly purified HA (2 to 200 µg/ml) to the culture medium of the transfected cells. At the end of 7 days, no obvious difference was apparent in the cell number of either cell type (data not shown). Thus, the presence of free HA by itself does not
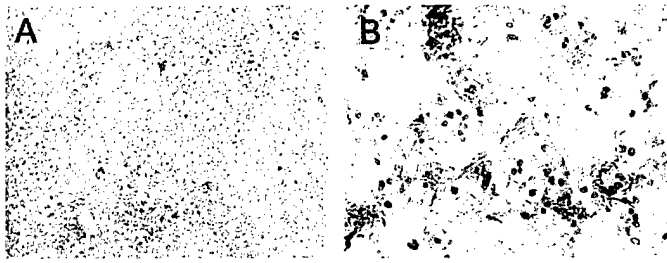
Fig. 4. Histochemical staining of control and HAS3-transfected TSU cells for HA using a biotinylated HA binding probe from cartilage. High density cultures were fixed, and incubated with b-HABP, followed by peroxidase labeled streptavidin and finally a substrate that gives rise to a red reaction product. A. A high density culture of control-TSU cells reveals a cobble stone appearance characteristic of cells exhibiting contact inhibition of growth . These cells have very little HA staining associated with them. B. A high density culture of HAS3-TSU cells reveals the presence of multilayered clusters of cells indicative of diminished contact inhibition of growth. Most of the HA staining was associated with these clusters.

Fig. 6. Growth of control and HAS3-TSU cells on the chicken CAM. Control and HAS3-transfected cells were placed on the CAMs of 10 day-old chicken embryos (1×10^6 cells/egg) and incubated at 37 °C. Five days later, the xenografts were removed and photographed: top panel, control-TSU cells; lower panel, HAS3-TSU cells.
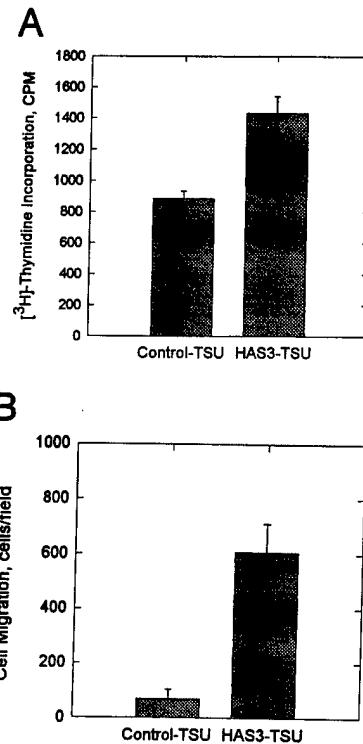

Fig. 5. Effects of conditioned medium on the proliferation and migration of endothelial cells. A. Cultures of ABAE cells were grown in the presence of conditioned from either control- or HAS3-TSU cells. After 36 hr [^{3}H]-thymidine was added to the medium for 8 hours, the cells were harvested and the amount of incorporated radioactivity was determined. The conditioned medium from the HAS3-TSU cells had a greater stimulatory effect on the proliferation of the ABAE cells than that of the control-TSU cells. B. To examine cell migration aliquots of ABAE cells were added to a 48 well Boyden chamber, allowed to attach to a Nucleopore membrane and then conditioned medium was added to the wells on the opposite side of the membrane. After 2 hours, the cells that had migrated across the filter were stained, and enumerated (10 random fields were counted). The conditioned medium from the HAS3-TSU cells stimulated the migration of the endothelial cells to a greater extent than that from the control-TSU cells.

stimulate the cell growth under these conditions and suggests that increased levels of HA secreted into the medium does not act in an autocrine or paracrine fashion to stimulate the growth of these cells. A more likely explanation is that the cell-associated fraction of HA (cell surface or cytoplasmic) plays a more important role in regulating the growth of these cells at high density.

1.4. Effect of Conditioned Media from HAS3-TSU on Endothelial cells: Since several studies have reported that under certain conditions, HA can modulate angiogenesis (30, 31) we examined the effects of conditioned medium from HAS3-TSU cells on the behavior of cultured endothelial (ABAE) cells. As shown in Fig. 5 A, conditioned medium from HAS3-TSU cells stimulated the proliferation of the ABAE cells by 66% as compared to that from control cells as judged by ^{3}H-TdR incorporation. Furthermore, the conditioned medium from the HAS3-TSU also stimulated the migration of ABAE cells through Nucleopore filters as compared to medium from that from control cells by more than 600% (Fig. 5 B). These results further suggest that the excess of HA produced by HAS3 in conditioned media from TSU cells could exert the stimulatory function on endothelium and is consistent with the early studies of West and coworkers (30, 31).

1.5. Growth of HAS3-TSU Cells on the CAM: Next, we compared the growth characteristics of the control and HAS3 transfected cells on the CAM of chicken eggs. In this experiment, equal numbers of the transfected TSU cells were placed on the CAMs of 10 day-old chicken embryos and allowed to grow for 5 days. As shown in Fig. 6, at the end of this period, the xenografts showed a striking divergence in their morphology. The control TSU cells formed rounded, nodular xenografts, with necrotic tissue in the center. In contrast, the HAS3-TSU cells gave rise to xenografts with a dispersed or spread-out morphology and without any obvious necrosis (Fig. 6). The HAS3-TSU xenografts were also 156 % larger than those of the control-TSU cells (Table 1). These results suggest that over-expression of HA enhances the tumor growth on CAM system.

1.6. HAS3 Promotes TSU Growth in Nude Mice. The results from chicken CAM were further tested with nude mice. In this system, transfected cells were injected subcutaneously into nude mice (male, 5 week-old). Again, the xenografts formed by the HAS3-TSU cells grew at a faster rate and appeared to be more vascularized than the control cells. After 3 weeks of growth, the HAS-3 xenografts were 3 times larger than those formed by the control cells (Fig. 7, Table 1). This suggests that HAS3 promotes the growth of TSU tumor cells in mice and is consistent with the results from the chicken CAM system.

However, when transfected cells were injected via tail vein into nude mice (5 mice/group), no lung metastasis was detected with either cell line. Thus, the over-expression of HA by itself is not sufficient to induce the metastatic behavior in these cells.

1.7. HAS3 Increases Intercellular Space and Angiogenesis in HAS3 Xenografts. Histological examination of the xenografts from nude mice revealed differences in their morphology (Fig. 8). While the xenografts varied from region to region, in general, the cells in the control-TSU xenografts were relatively homogeneous, compact and most of the HA appeared to be present in the cytoplasm of the cells (Fig. 8 A). In contrast, the HAS3-TSU cells formed small clusters or nests of cells that were surrounded by a matrix rich in HA (Fig. 8 B). Such structures were not observed in the control-TSU xenografts.

The extent of angiogenesis in these xenografts was examined histochemically staining for endothelial cells (anti-CD31). The HAS3-TSU xenografts demonstrated stronger staining for endothelial cells as compared to the control-TSU xenografts. The number of vessels in random 10 high-power fields in the

Table 1. The growth of transfected TSU cells in the chicken CAM and in the nude mouse. The TSU cells were grown on the CAM for 5 days were carefully removed and weighed. In nude mouse model system, the TSU cells were grown for 22 days and the volumes were determined.

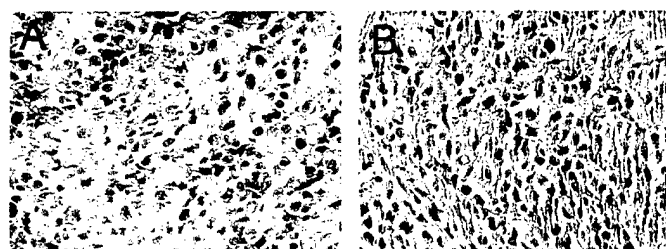| | Xenograft | | |
	Control-TSU	HAS3-TSU	% Increase
Chicken CAM (5 days)	59.1±5.6 mg	151.3±23.7 mg	156
Nude Mice (22 days)	0.063±0.016 cm³	0.311±0.049 cm³	394

Control-TSU

HAS3-TSU

Fig. 7. Xenografts of control and HAS3 transfected TSU cells in nude mice. Nude mice were injected with 2 x 106 control- and HAS3-TSU cells. Twenty-two days later, the xenografts were harvested and photographed: top panel, control-TSU cell; lower panel, HAS3-TSU cells.

Fig. 8. The distribution of HA in xenografts formed by transfected TSU cells in nude mice. The xenografts were fixed in formalin, processed for histology and the resulting paraffin sections were stained for HA (red) using b-HABP and counter-stained with hematoxylin (blue). A. A representative section of a control-TSU xenograft shows that cells are compact and most of the HA staining is associated with the cytoplasm of the cells. B. A representative section of a HAS3-TSU xenograft reveals that cells are present in small clusters, surrounded by a stroma rich in HA. While the microscopic morphology of the xenografts varied from region to region, the HA-rich stroma was prevalent in the HAS3-TSU cells and absent from the control-TSU cells.

samples of HAS3-TSU xenografts was 138% higher than that from control-TSU cells (169 in Control-TSU xenografts vs. 403 in the HAS3-TSU xenografts). This suggests that increased levels of HA can stimulate angiogenesis in these cell and this may, in part, account for the faster growth rate.

1.8. Interpretation of Results: In this study, we have characterized human HAS3 with regard to both its structure and its function in tumor progression. Based upon its deduced amino acid sequence, HAS3 shares significant homology with HAS1 and HAS2, and contains a signal peptide as well as six transmembrane regions strongly suggesting that it associated with the plasma membrane. Its enzymatic activity was demonstrated by the fact that transfection of TSU cells with expression vectors resulted in increased production of HA as determined by histochemical staining, dot blot analysis and quantitative ELISA. These findings are consistent with earlier studies of HAS proteins (12-19).

This study also suggests that stimulation of HA synthesis in TSU cells by transfecting them with HAS3 expression vectors enhanced their growth in both chicken embryos and in nude mice. Furthermore, this enhanced tumor growth appears to be due to two distinct mechanisms. The first mechanism involves a direct effect on the tumor cells themselves as suggested by the fact that in tissue culture, HAS3 transfected cells grew at a faster rate at high density. The second mechanism promoting tumor growth rate results from an increase in vascularization as reflected by the greater density of blood vessels present in xenografts of transfected cells in nude mice. Together, these two factors contribute to the increased tumor growth rate.

While HAS3 stimulates the production of both secreted and cell-associated HA, it is this latter fraction that appears to be most important in modulating cell growth in culture. This was suggested by the observation that addition of free HA to the cell medium did not result in increased proliferation that was seen in the HAS3 transfected cells. Thus, the most likely explanation is that it is the cell-associated pool of HA that is responsible for the biological effects on proliferation. This cell-associated fraction of HA consists of that present in the cytoplasmic as well as on the cell surface, either or both of which could be responsible for the increase in proliferation.

The HA on the surface of the cells can form a pericellular coat which can be directly visualized by its ability to exclude small particles such as erythrocytes (32). The size of this coat is due in part to small, microvilli-like projections that extend out from the surface of the cells to which the HA is attached (33). This pericellular coat could stimulate the growth of cells by several different mechanisms. One possible mechanism is that it disrupts intercellular junctions and thereby allows the cells to detach from the substrate so that they can divide and occupy new space (34-36). This would allow cells to overcome contact inhibition of growth which is characteristic of TSU cells and allow them to from multi-layers at high density cultures as we have observed. Another possible mechanism by which pericellular HA could stimulate proliferation is by maintaining spaces between cells that increases the flow of nutrients. Indeed, the larger extracellular space apparent in xenografts of HAS3 transfected cells in nude mice could serve as conduits through which nutrients could diffuse to support cells located some distance from the blood supply and thus facilitate their growth. Presumably, the

HA also appears to promote vascularization which is clearly important in regulating tumor growth (37-40). This was indicated by our observation that in xenografts of HAS3-TSU cells formed in nude mice, there was an increase in the density of blood vessels as compared to the control cells as determined by histochemical staining for endothelial cells (CD31). Part of this increased vascularization may be due to the pericellular spaces generated by the HA provides space which facilitates the migration and invasion of

endothelial cells. In addition, the HA itself can stimulate the migration of endothelial cells. This was also indirectly suggested by experiments showing that conditioned media from the HAS3 transfected cells stimulated the growth and migration of cultured endothelial cells. This is consistent with earlier studies of West and his associates have shown that oligosaccharide fragments of HA stimulate the formation of new blood vessels in the chorioallantoic membrane of chicken embryos (30, 31).

While the results of this suggest that over-expression of HAS3 in TSU prostate cancer cells promotes their tumorigenicity, there are some aspects of the present study that appear to contradict the results of other studies. For example, while we found that TSU transfectants grew faster in culture, Kosaki and coworkers found no such increase in the growth of HT1080 cells transfected with HAS2 under anchorage dependent conditions, although these cells did form bigger colonies in suspension culture (20). In addition, while we found increased stroma and angiogenesis in xenografts of HAS3-TSU cells in nude mice, Kosaki *et al.* found no such increase in HAS2 transfected HT1080 cells (20). We believe that these difference may due in part to the different target cells that were employed in these studies. The TSU cells employed in this study are of epithelial origin, while HT1080 cells are derived from a fibrosarcoma of connective tissue cells. This could account for the differences see with regard to growth behavior and the production of HA in the connective tissue, and their ability to stimulate angiogenesis. Alternatively, the differences could be attributed to the characteristics of the HA synthases that were used in the transfection, since they differ with respect to both their synthetic activity as well as the size of the HA that they produce (16-18).

Another apparent discrepancy was our observation that transfection of TSU cells with HAS3 did not appear to stimulate their ability to form lung metastases in nude mice. In contrast, we had previously reported that the levels of HA on cell surface of B16 cells was directly correlated with their metastatic behavior (3). Similarly, Itano *et al.* found that transfection of FM3A with HAS1 enhanced their metastatic properties (21). Again, we believe that these divergent results are due to the different cell types that are used as targets for transfection. In the case of B16 and FN3A, these cell lines originally possess the ability to undergo metastasis, and stimulation of HA synthesis in these cells enhance this innate property. In contrast, TSU cells appear to lack this ability (at least in nude mice) and increased HA synthesis, by itself, is not sufficient to promote metastatic properties. Clearly, the process of metastasis is a complex phenomenon involving the collaboration of many molecules. While the production of HA is one of the factors, it is not sufficient for the tumor metastasis.

In conclusion, the results of this study indicates that HA expression plays a role in tumor progression and are consistent with earlier studies demonstrating a correlation between HA levels and tumorigenicity. Furthermore, the HA may be acting through several different mechanisms, including: 1, a direct effect on the growth of the tumor cells themselves; 2, the formation of extracellular conduits through which nutrients can flow; and 3, the stimulation of blood vessel growth. However, these effects depend upon the particular cell type and the specific environment. Given the complexity of the effects of HA, it may be difficult to predict exactly how HA will influence the behavior of tumor cells. In any case, HA be more of a facilitator or promoter of tumor growth than an instigator.

TASK 2. The Effects of Decreased HA Expression on Tumor Growth: If our working hypothesis that HA promotes tumor cell growth is correct, then blockade of HA production should inhibit malignant progression. To test his possibility, we have proposed to transfected TSU prostate cancer cells with the vectors that drive the expression of anti-sense RNA for these genes. The anti-sense RNA binds specifically to the mRNAs for HA synthase, targets these molecules for degradation and inhibit the normal translation of HA synthase. The resultant will then examined for phenotype changes with regard to growth rate in tissue culture, and in animal models (chicken CAM and nude mice).

2.1. Transfection of Tumor Cells with Vectors for the Antisense of HA Synthase: Anti-sense sequences for HAS3 were ligated into the pcDNA3 vector (Invitrogen) and amplified in bacteria. Both anti-sense and control plasmids were isolated and used to transfect TSU cells using the Ca precipitation method. Transfected clones were selected by their ability to survive in 1 mg/ml of G418. To avoid complications associated with clonal variations, all of the surviving clones were pooled and expanded for experimental analysis throughout this study. It was our hope that since the anti-sense sequence to HAS3 was very similar to that of HAS1 and 2, that all three forms of HA synthase would be down-regulated.

2.2. Characterization of Transfected Cells: In initial experiments, the transfected cells were tested for the expression of HA. To do this, we collected the conditioned media from the cells and extracted the cell layer with detergents. These samples were then assayed for HA using a modified ELISA assay using a biotinylated HA-binding probe isolated from cartilage (b-HABP). As shown in Fig. 9 A, the TSU cells transfected with the anti-sense HAS3 vector had approximately one third the amount of HA in the cell layer as that in their vector-transfected counterpart. These cells also secreted less HA into the medium (Fig. 9. B), but the magnitude of this difference was not as great as with the cell layer. This may be a reflection of the fact that HAS3 produces a greater proportion of cell-associated than secreted HA as compared to the other HA synthases. Thus, if HAS3 is preferentially down-regulated then the cell-associated HA should would be expected to show a greater response.

The down regulation of cell-associated HA was also apparent when the cells were stained histochemically for HA with b-HABP. Both vector and anti-sense transfected TSU cells were cultured at low density, fixed briefly in formaldehyde and then stained for HA using b-HABP (red color) and counter-stained with hematoxylin (blue). Figure 10 A and B shows that the anti-sense transfected cells stained less intensely than the vector (control) cells, suggesting that they had less HA. These results were consistent with the ELISA assays described above.

2.3. The Growth Rates of Transfected TSU Cells In Vitro: Next, we examine the growth rates of the control and anti-sense transfectants in tissue culture. For this equivalent numbers of cells were subcultured into 24 well plates and at different time points thereafter, wells were harvested with a solution of EDTA and the cell number was determined with a Coulter Counter. Figure 11 shows that the anti-sense HAS3 transfected TSU cells grew much slower than their control counterparts (vector transfected). This difference was unexpected, and at present we do not know why the down regulation of HAS3 has such a dramatic effect on the growth rates of these cells. This observation deserves further investigation.

2.4. Examine the Effect of Anti-sense HAS3 on Tumor Growth In Vivo: In this set of experiments, we examine the growth of the control and anti-sense HAS3 TSU cells in animal models consisting of both the chicken embryo CAM and nude mice. In the first experimental model, samples containing approximately
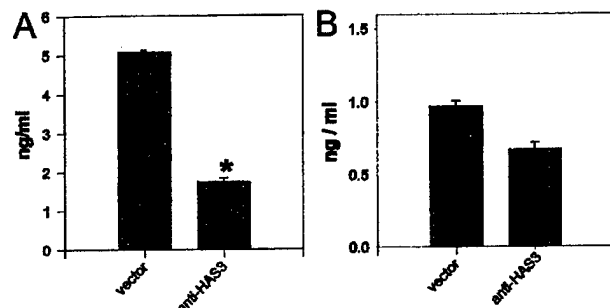
Fig. 9. The production of HA by control and anti-HAS3 transfected TSU cells. **(A)** Detergent lysates of the cells were assayed for HA using an ELISA employing b-HABP from cartilage. The cells transfected with the vector alone (control) had greater levels of HA than those transfected with anti-HAS3. **(B)** The conditioned medium from these cells show a similar pattern but the difference was not as great.

Fig. 10. Histochemical staining of transfected TSU cells in tissue culture. Both the control **(A)** and anti-HAS3 **(B)** transfected cells were cultured at low density, fixed and stained with b-HABP from cartilage for HA (red color) and counter-stained with hematoxylin (blue color). The cytoplasm of the control cells stained more intensely for HA than did those transfected with anti-sense for HAS3.

Fig. 11. The growth rates of vector and anti-HAS3 transfected TSU cells in tissue culture. Cells were subcultured at equal densities, and at the indicated times thereafter, harvested with EDTA and the cell number was determined with a Coulter Counter. The TSU transfected with the anti-HAS3 grew much slower than their control counterparts.
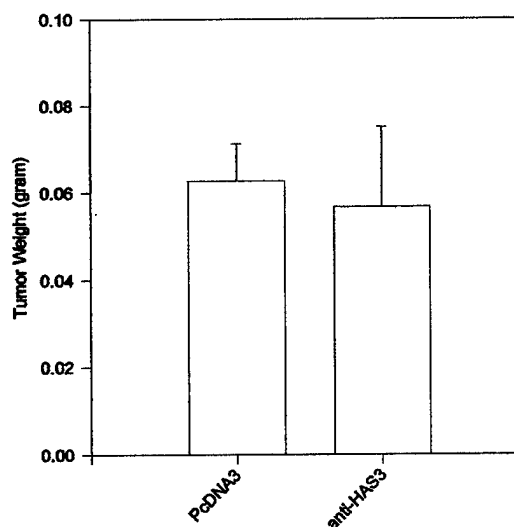
Fig. 12. The growth of vector and anti-HAS3 TSU cell on the CAM of chicken embryos. Equal numbers of control and anti-HAS3 cells were applied to the CAMs of 10 day old chicken embryos and harvested 5 days later. The final weights of the xenografts show that there was not a significant difference between the cells under these conditions.

2×10^6 cells were placed on the CAM of 10 day old chicken embryos and allowed to grow for 5 days. At the end of this time, the tumor xenografts were removed and weighed. Figure 12 shows that there was no obvious difference in the weights of the tumor xenografts at the end of the experiment. Thus, in the chicken CAM model system, the down regulation of HAS3 did not appear to influence the growth rate of the cells. However, it should be mentioned that the CAM model system is not representative of the growth conditions that tumor cells normally encounter *in vivo*. For example, the CAM is already highly vascularized and the cells are exposed to the air which allows for oxygen to diffuse into the tumors.

In the final experiment, we examined the growth of these cells in the nude mouse, which more closely approximates the conditions that tumor cells encounter *in vivo*. For these experiments, 5×10^5 control and anti-sense TSU cells were injected sq. into nude mice, and the size of the resulting xenografts was followed by measurement with calipers. Figure 13 shows that under these condition, the anti-sense HAS3 cells grew much slower than their control counterparts. Thus, under the conditions that tumor cells would encounter in vivo, the down-regulation of HAS3 cause a reduction in tumor growth rate. These results are consistent with our working hypothesis that HA synthesis promotes tumor progression.

Fig. 13. The growth rates of control and anti-HAS3 transfected TSU cells in nude mice. Approximately 2 $\times$ 10^6 transfected TSU cells were injected subcutaneously into nude mice and the resulting xenografts were measured at the indicated time points. The control TSU cells grew much faster than those transfected with the anti-HAS3 vector.

2.5. Interpretation of Results: On the whole, the results of these experiments tended to support our hypothesis that HA synthesis promotes tumor growth. In particular, the growth of these cells in the nude mouse showed that down regulation of HAS3 resulted in a much slower growth rate. However, other aspects of these studies were not completely consistent. For example, there was no obvious difference in the growth of these cells on the CAM, which may be due to the radically different conditions between these two assay systems. In addition, the fact that there was a major difference in the growth of these cells in tissue culture suggests that the down-regulation of HAS3 may be influencing other aspects of cell physiology in addition to the production of HA in the extracellular matrix. The nature of these effects should be addressed.
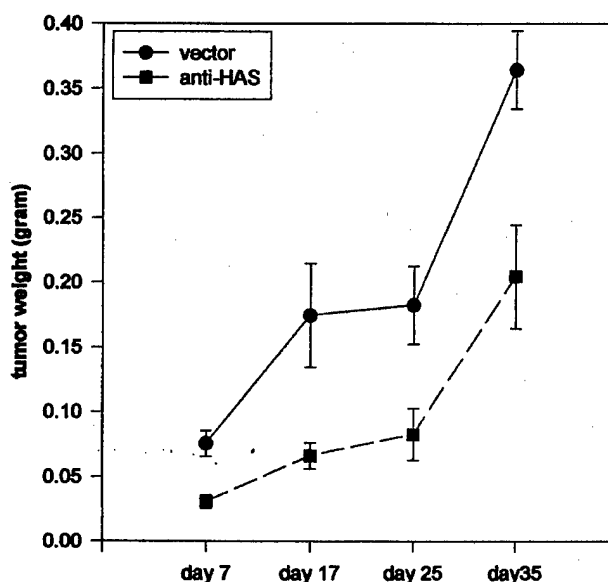
TASK 3. The Effect of Hyaluronidase on the Growth of Tumor Cells: In this final task, we examined the effects of reducing the levels of HA on the growth of tumor cells. We had initially proposed to do this by transfecting tumor cells with an expression vector for HAase (sperm-type and membrane-bound, PH-20). Unfortunately, we were unable to detect any increase in HAase activity in the transfected cells suggesting that the recombinant protein was not active. Consequently, we have dropped this approach in favor of a new one in which we examined the effects of HAase on tumor xenografts growing on the chorioallantoic membrane of chicken embryos. We anticipated that the removal of HA from the tumors would inhibit the growth of these cells by causing the collapse of pericellular spaces through which nutrients diffuse. To our surprise, we found that treatment with HAase stimulated the apparent growth of the xenografts. Further experimentation revealed that much of this increase appeared to be due to formation of hemorrhagic regions within the xenografts.

3.1. Effect of HAase on the growth of tumor cells on the chicken CAM: In initial experiments, we examined the effects of testicular HAase on the growth of B16B16 and TSU tumor cells on the CAM of chicken embryos. For this assay, we placed a set number of tumor cells on the CAMs of 10 day old chicken embryos and two days later injected HAase or control preparations (saline or heat-inactivated HAase) into the blood vessels of the CAM. After a total of 7 days of growth, the resulting xenografts were collected for further examination. While the single treatment with HAase did not have a significant effect on the growth of TSU cells (data not shown), it had a profound effect on the growth of the B16B16 cells under these conditions. As shown in Fig. 14 A, the B16B16 xenografts from the HAase treated embryos were significantly larger than those from the control embryos. This fact was also reflected in the weights of the xenografts as shown in Fig. 14 B, demonstrating that a single treatment with HAase increased the final mass of the xenograft by one to two fold, and this effect was reversed if the testicular HAase preparation was heat inactivated. It is important to note that both testicular and *Streptomyces* HAase enhanced the growth of the B16B16 tumor cells, since these two enzymes differ in their enzymatic specificity. While testicular HAase can degrade both HA and chondroitin sulfate, *Streptomyces* HAase is specific for HA (41). Thus, the fact that both of these enzymes had similar effects on the growth of the B16B16 cells strongly suggested that they were mediated through the degradation of HA.

3.2. Effect of HAase the growth of B16B16 cells in tissue culture: The stimulatory effects of HAase on B16B16 growth on the chicken CAM could be due to either a direct effect on the tumor cells themselves or to some host mediated response to the cells. To distinguish between these two possibilities, we examined the effects of HAase on the growth of B16B16 cells in tissue culture. For this cells were grown in complete media in the presence of testicular HAase or a heat-inactivated preparation as a control and at various times, the number of cells was determined with a Coulter counter. As shown in Fig. 15, the testicular HAase did not have a significant effect on the growth of B16B16 cells in culture. A similar lack of response was obtained with cultured TSU cells as well (data not shown). Clearly, HAase does not stimulate the growth of B16B16 cells in tissue culture suggesting that its effect on the growth of the B16B16 xenografts was probably due to an indirect effect on some other aspect of the tumor growth.

3.3. Histology of the B16B16 xenografts: To further explore the mechanism by which HAase stimulated the growth of B16B16 cells on the CAM, we examined the histology of these xenografts. Staining with hematoxylin and eosin revealed obvious differences in the morphology of control and HAase treated xenografts (see Fig. 16). In the case of the control xenografts, they were relatively uniform in composition with small blood vessels coursing through the mass (Fig. 16 A). In contrast, the xenografts from chickens treated with either testicular or *Streptomyces* HAase consistently contained regions of sinusoid-like structures containing erythrocytes interspersed with cords of tumor cells (Fig. 16 B). Typically, these
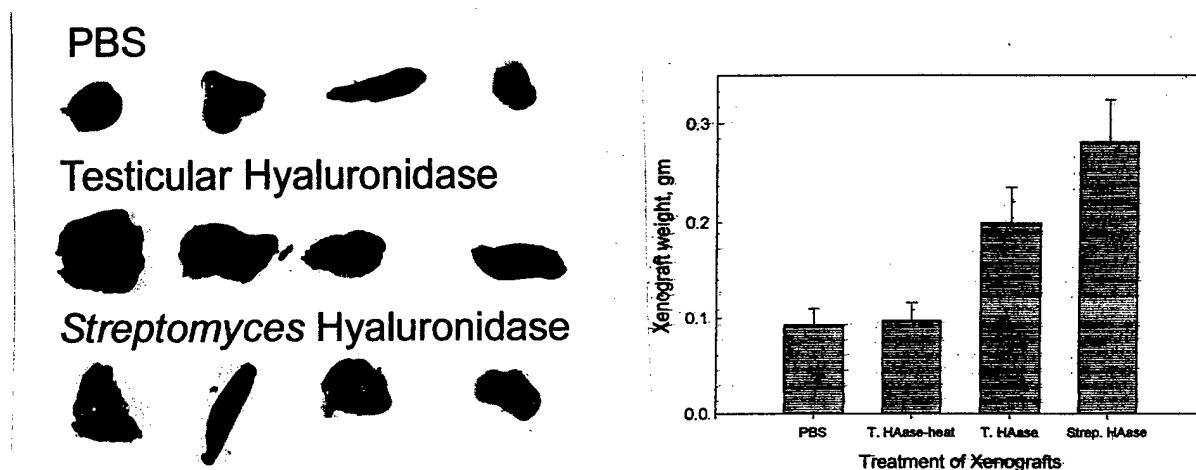
Fig. 14. Effect of hyaluronidase on the growth of B16B16 cells on the CAM of chicken embryos. For this experiment a suspension of B16B16 cells was applied to the CAMs of 10 day old chicken embryos and allowed to grow for 2 days before the embryos were given iv injections of hyaluronidase. After seven days the resulting xenografts were harvested. (A) A photograph of representative xenografts from eggs that had been treated with saline (top row), testicular hyaluronidase (middle row) and *Streptomyces* hyaluronidase (bottom row). Those treated with active hyaluronidase were larger than the saline controls. It should also be noted that while the control xenografts were flat, those treated with hyaluronidase grew out of the plane of the CAM. (B) The weights of xenografts shows that treatment with both testicular and *Streptomyces* hyaluronidase resulted in heavier xenografts than those treated with saline or heat-inactivated testicular hyaluronidase. (n = 9 or 10; Bars = standard error of the mean)

Fig. 15. The effect of hyaluronidase on the growth of cultured B16B16 cells. The cells were subcultured into 24 well dishes in complete medium containing 10 μg/ml of testicular hyaluronidase or heat- inactivated preparations as a control. At the indicated times, the cell were harvested in a solution of EDTA and the cell number was determined with a Coulter counter. Treatment with hyaluronidase did not have an obvious effect on the growth rate of these cells in culture. (Bars = standard error of the mean)
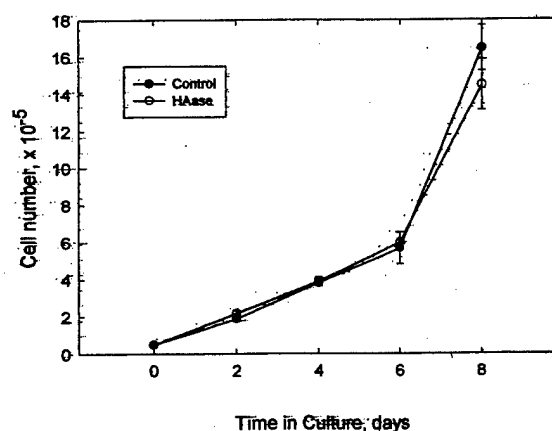
regions were located in the center of the tumor mass and were surrounded by tumor masses similar in morphology to that of the controls.

The differences between the control and the HAase-treated xenografts was confirmed by biochemical measurements. Representative xenografts were homogenized and assayed for hemoglobin as a measure of erythrocyte content. As shown in Fig. 17, the hemoglobin content of the xenografts from the HAase-treated embryos was significantly higher than that from the controls. Thus, at least part of the increased size of the xenografts is due to a greater amount of blood in the tissue, while the remainder is probably due to an increase in the number of tumor cells themselves.

3.4. Distribution of HA: To further evaluate the HAase-induced formation of sinusoidal cavities, we examined the distribution of HA in the B16Bl6 xenografts. Sections of the control xenografts (i.e. not treated with HAase) were stained for HA with a binding complex isolated from cartilage (b-PG). Figure 18 shows that HA staining (in red) was present within the mass of B16Bl6 cells around nodules (or nests) of the tumor cells. In addition, HA was also apparent in perivascular regions. When HAase treated xenografts were examined histologically, little or no HA was apparent near the sinusoidal cavities in the center of the tumor mass (data not shown). However, HA was detected towards the edge of the xenograft where newly proliferating tumor cells were present similar to that of the untreated xenografts. These results suggests that the i.v. injection of HAase digests the HA located around the blood vessels and between the nests of tumor cells, and this, in turn, creates new spaces through which the blood may flow to nourish the tumor cells.

3.5. Distribution of endothelial cells: An important question is whether the sinusoidal cavities present in the HAase-treated xenografts represented legitimate blood vessels or simply spaces in which blood has pooled. In other words, are these spaces lined by endothelial cells? To address this question, sections of the tumor were stained with an antibody directed against chicken endothelial cells (Paris#1). However, no positive staining could be detected surrounding the cavities (data not shown). In addition, Western blotting of extracts from the xenografts with the antibody did not show any significant increase in this maker in the HAase-treated versus the control xenografts.

Next, we examined the patency of these sinusoidal cavities. To accomplish this, a small amount of India ink was injected into the chicken embryos approximately 20 min prior to collection of the xenografts. As shown in Fig. 19, the India ink demonstrated the presence of small blood vessels coursing throughout the xenograft. However, very little of the India ink was associated with the sinusoidal cavities, and the few positive regions were confined to small regions within the cavities. These results suggest that the sinusoidal cavities induced by HAase treatment are not true blood vessels, but rather simply spaces in which blood has pooled. While melanoma cells are able to take on the properties of endothelial cells under some circumstances (42), this does not appear to be the case here since blood is not actively circulating through these spaces. Despite this fact, these cavities could serve as conduits to increase the diffusion of nutrients to the tumor cells in these regions.

3.6. Interpretation of Results: The major conclusion of this study is that the systemic injection of HAase caused the formation of hemorrhages in xenografts of some tumor cells. This was initially indicated by the fact that histological examination of B16Bl6 xenografts treated with either testicular or *Streptomyces* HAase revealed the presence of sinusoids containing blood that were absent from control xenografts. This

Fig. 16. Sections of B16Bl6 xenografts stained with hematoxylin and eosin. The xenografts from both control embryos (saline injected) and those injected with hyaluronidase were processed for histology and stained with hematoxylin and eosin. (A) A representative section through a control xenograft shows that B16Bl6 cells are arranged in a compact mass containing little connective tissue and with small blood vessels coursing through the mass. The density of the blood vessels was consistent across the mass of tumor cells. (B) A representative section of a B16Bl6 xenograft that had been treated with hyaluronidase shows that the central portion of the mass contains large, irregularly-shaped sinusoids that were filled with blood cells. The more peripheral region of the mass was similar in morphology to that of the control xenograft which was compact and contained numerous small blood vessels. (Bar = 20 μm)
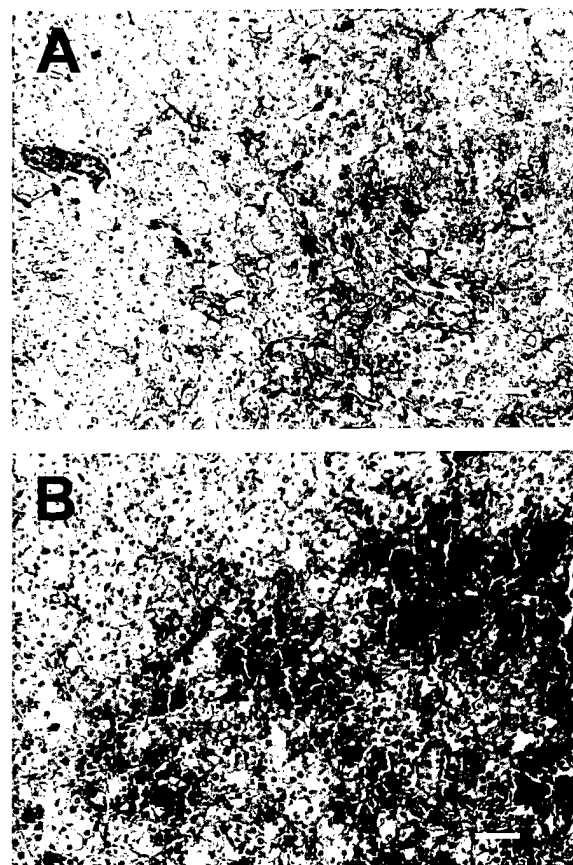
Fig. 17. Hemoglobin content of xenografts. Samples of both the control xenografts and those from animals treated with testicular hyaluronidase were homogenized and analyzed for hemoglobin content. The hemoglobin content of the xenografts treated with hyaluronidase were higher than the controls that had been treated with either saline or heat-inactivated hyaluronidase. (n = 3)
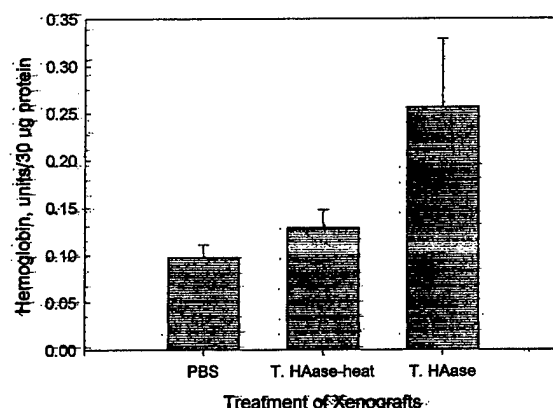
Fig. 18. Histological staining of B16Bl6 xenografts for hyaluronan. Sections of B16Bl6 xenografts from control animals (i.e. not treated with hyaluronidase) were stained for hyaluronan using a biotinylated binding complex from cartilage (b-PG) followed by peroxidase conjugated to peroxidase and finally a peroxidase substrate that gives rise to a red reaction product. The sections were counter-stained with hematoxylin. Hyaluronan was localized to perivascular regions of the larger blood vessels located at the periphery of the xenografts (short arrows) and in the stroma of the tumor surrounding small nodules of the tumor cells (long arrows).
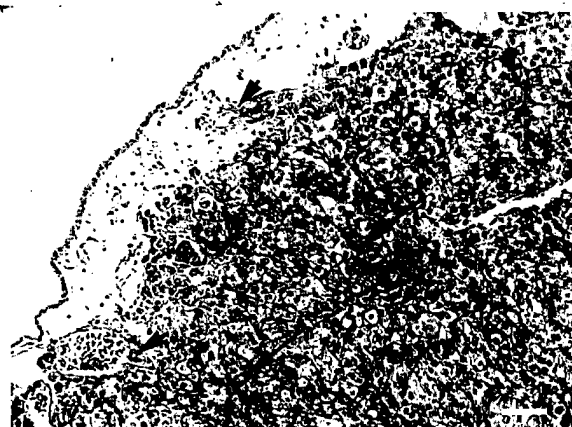
Fig. 19. Section of a B16B16 xenograft following injection of India ink. B16B16 cells were applied to the CAM of chicken embryos which were then injected with testicular hyaluronidase as described in the Materials and Methods section. Twenty min prior to harvesting, the embryos were injected with India ink to serve as a marker of blood flow. The resulting xenografts were processed for histology and stained with hematoxylin and eosin. While the India ink was apparent in the smaller blood vessels that course through the xenograft, it was not detected in the sinusoids suggesting that they were not patent. It should be noted that in some cases, that India ink was present in small blood vessels located entirely within the sinusoids (indicated by arrow).
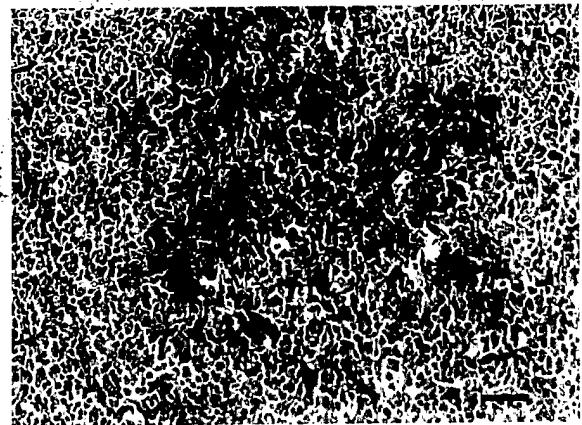
observation was also supported by biochemical analysis of the xenografts indicating that those that had been treated with HAase had a higher content of hemoglobin than their control counterparts. Moreover, these sinusoidal spaces did not appear to be functional blood vessels because they were not lined by endothelial cells as indicated by histochemical staining and they were not patent since they did not become filled with India ink that had been injected into the blood shortly before harvesting. Taken together, these results indicate that HAase can cause internal bleeding in the B16B16 xenografts and this is at least in part responsible for the increased size of these xenografts as compared to the controls.

The most likely explanation for these effects is that the HAase degraded the HA in the perivascular regions that was important for maintaining the structural integrity of the blood vessels and tumor tissue. When the injected HAase entered the blood vessels associated with the B16B16 xenografts, it escaped into the surrounding tissue where it degraded both the HA that helps maintain the structure of the blood vessels as well as the spaces between clusters of B16B16 tumor cells. This is in keeping with our histochemical observations that HA is located in these regions. Presumably, the hemorrhages formed shortly after the injection of HAase and subsequently the tumor cells continued to grow around the periphery resulting in a solid tumor mass surrounding a core hemorrhagic area. The increased size of the HAase-treated xenografts resulted in part from an increase in the blood supply as well as increased growth of the cells. It should be noted that while this effect did not occur with all of tumor xenografts tested, in particular TSU cells did not show a similar response. Thus, tumor cells differ in their response to treatment with HAase.

It should be noted that the results reported here are exactly opposite of what we had originally expected. According to our working hypothesis, the removal of the pericellular HA should have inhibited tumor growth by preventing the diffusion of nutrients. While these results.are not in accord with our expectations, they do not necessarily contradict our original working hypothesis. Rather they show that HA plays a structural role in maintaining the integrity of blood vessels associated with tumors. . It would be of interest to investigate the mechanism by which HA is able to carry out this function. Indeed, it may be possible to take advantage of this phenomenon to target certain types of tumors.

ACRONYMS AND SYMBOL DEFINITIONS

b-HABP	Biotinylated proteoglycan - used as a specific staining probe for hyaluronan.
CAM	Chorioallantoic membrane
CD44	Cluster of determination (differentiation) - same as the hyaluronan receptor or binding site.
CMF-PBS	Calcium and magnesium free phosphate buffered saline.
DMEM	Dulbecco's modifed Eagle's medium
HA	Hyaluronan.
HAase	Hyaluronidase (either testicular or *Streptomyces*)
HAS3	Hyaluronan synthase, isoform 3
mAb	Monoclonal antibody.
HABP	A complex of a trypsin fragment of cartilage proteoglycan and link protein that binds to HA with high affinity and specificity.

KEY RESEARCH ACCOMPLISHMENTS:

- The cDNA for human HAS3 was cloned and characterized. The open reading frame consisted of 1,659 base pairs coding for 553 amino acids with a deduced molecular weight about 63 kDa and isoelectric pH of 8.70. The sequence of human HAS3 displayed a 53% identity to HAS1 and 67% identity to HAS2. It also contained a signal peptide and 6 potential transmembrane domains, suggesting that it is associated with the plasma membrane.

- To evaluate the physiological role of human HAS3, expression vectors for this protein were transfected into TSU cells (a prostate cancer cell line). The over-expression of HA in the transfected cells was confirmed by histochemical staining, dot blot analysis and ELISA.

- The HAS3-TSU cells were found to differ from their control transfected counterparts with respect to the following: 1) they grew at a faster rate in high (but not low) density cultures; 2) conditioned media from these cells stimulated the proliferation and migration of endothelial cells; 3) when placed on the chorioallantoic membrane of chicken embryos, these cells formed large, dispersed xenografts while the control transfectants formed compact masses; and 4) when injected subcutaneously into nude mice, the xenografts formed by HAS3 transfectants were bigger than those formed by control transfectants.

- Histological examination of these xenografts indicated that the HAS3 transfectants had increased intercellular space rich in HA, and a greater number of blood vessels.

- The HAS3 transfected TSU cells did not show an increase in their metastatic properties as judged by their ability to form lung metastases following i.v. injection.

- Transfection of TSU cells with anti-sense sequences to HAS3 results in a down regulation of HA production.

- The anti-sense HAS3 TSU cells grew slower in tissue culture and in nude mice than their control counterparts. On the other hand there was no apparent difference in the growth rate of the transfected cells when grown on the CAM of chicken embryos. While the results are not entirely consistent, on the whole they tend to support the working hypothesis that HA promotes tumor progression.

- The size of some tumor xenografts growing on the CAM of chicken embryos was increased by the i.v. injection of HAase.

- The treatment of tumor xenografts with HAase resulted in the formation of hemorrhages suggesting that HA plays role in maintaining the integrity of blood vessels.

REPORTABLE OUTCOMES:

Liu, N., Gao, F., Han, H., Xu, X., Underhill, C. B. and Zhang, L. Hyaluronan Synthase 3 Overexpression Promotes the Growth of TSU Prostate Cancer Cells. *Cancer Research* 61:5207-5214.

CONCLUSION AND SIGNIFICANCE:

- These results suggest that the HAS3-induced over-expression of HA promotes tumorigenicity by several different mechanisms, including: 1) a direct effect on the growth of the tumor cells, 2) the formation of extracellular conduits through which nutrients can flow, and 3) the stimulation of blood vessel growth. This is consistent with our original working hypothesis that an extracellular matrix of HA enhances tumor cell growth.
- The down-regulation of HA expression by anti-sense to HAS3 tends to decrease the growth rate of tumor cells in tissue culture and in nude mice. These results are also consistent with our working hypothesis that HA is involved in tumor progression.
- HA appears to play an important role in maintaining the structural integrity of blood vessels as demonstrated by the fact that treatment with HAase causes hemorrhages in some types of tumor xenografts.

REFERENCES:

1. Toole, B. P., Biswas, C., and Gross, J. Hyaluronate and invasiveness of the rabbit V2 carcinoma. Proc Natl Acad Sci U S A; *76:* 6299-303, 1979.
2. Kimata, K., Honma, Y., Okayama, M., Oguri, K., Hozumi, M., and Suzuki, S. Increased synthesis of hyaluronic acid by mouse mammary carcinoma cell variants with high metastatic potential. Cancer Res. *43:* 1347-1354, 1983.
3. Zhang, L., Underhill, C. B., and Chen, L. Hyaluronan on the surface of tumor cells is correlated with metastatic behavior. Cancer Res. 55: 428-433, 1995.
4. Marotta, M., D'Armiento, F. P., Martino, G., Donato, G., Nazzaro, A., Vecchione, R., and Rosati, P. Glycosaminoglycans in human breast cancer: morphological and biochemical study. Appl. Pathol. (Switzerland), *3:* 164-169, 1985.
5. Coppes, M. J. Serum biological markers and paraneoplastic syndromes in Wilm's tumor. Med. Pediatr. Oncol., *21:* 213-221, 1993.
6. Horai, T., Nakamura, N., Tateshi, R., and Hattori, S. Glycosaminoglycans in human lung cancer. Cancer, *48:* 2016-2021, 1981.
7. Roboz, J., Greaves, J., Silides, D., Chahinian, A. P., and Holland, J. F. Hyaluronic acid content of effusions as a diagnostic aid for malignant mesothelioma. Cancer Res., *45:* 1850-1854, 1985.
8. KoJima, J., Nakamura, N., Kanatani, M., and Omori, K. The glycosaminoglycans in human hepatic cancer. Cancer Res., *35:* 542-547, 1975.
9. Azumi, N., Underhill, C. B., Kagan, E. and Sheibani, K. A novel biotinylated probe specific for hyaluronate: Its diagnostic value in diffuse malignant mesothelioma. Amer. J. Surg. Pathol., *16:* 116-121, 1992.
10. Dahl, I. M. S., and Laurent, T. C. Concentration of hyaluronan in serum of untreated cancer patients reference to patients with mesothelioma. Cancer *62:* 326-330, 1988.

11. Frebourg, T., Lerebours, G., Delpech, B., Benhamou, D., Bertrand, P., Maingonnat, C., Boutin, C., and Nouvet, G. Serum hyaluronate in malignant pleural mesothelioma. Cancer; *59:* 2104-2107, 1987.

12. Shyjan, A. M., Heldin, P., Butcher, E. C., Yoshino, T., and Briskin, M. J. Functional cloning of the cDNA for a human hyaluronan synthase. J. Biol. Chem. *271:* 23395-23399, 1996.

13. Watanabe, K., and Yamaguchi, Y. Molecular identification of a putative human hyaluronan synthase. J. Biol. Chem. *271:* 22945-22948, 1996.

14. Itano, N., and Kimata, K. Molecular cloning of human hyaluronan synthase. Biochem. Biophys. Res. Commun. *222:* 816-820, 1996.

15. Itano, N., and Kimata, K. Expression cloning and molecular characterization of HAS protein, a eukaryotic hyaluronan synthase. J. Biol. Chem. *271:* 9875-9878, 1996.

16. Spicer, A. P., Olson, J. S., and McDonald, J. A. Molecular cloning and characterization of a cDNA encoding the third putative mammalian hyaluronan synthase. J. Biol. Chem. *272:* 8957-9861, 1997.

17. Spicer, A. P., and McDonald, J. A. Characterization and molecular evolution of a vertebrate hyaluronan synthase gene family. J. Biol. Chem. *273:* 1923-1932, 1998.

18. Spicer, A. P., and Nguyen, T. K. Mammalian hyaluronan synthases: investigation of functional relationships in vivo. Biochem. Soc. Trans. *27:* 109-115, 1999.

19. Itano, N., Sawai, T., Yoshida, M., Lenas, P., Yamada, Y., Imagawa, M., Shinomura, T., Hamaguchi, M., Yoshida, Y., Ohnuki, Y., Miyauchi, S., Spicer, A. P., McDonald, J. A., and Kimata, K. Three isoforms of mammalian hyaluronan synthases have distinct enzymatic properties. J. Biol. Chem. *274:* 25085-25092, 1999.

20. Kosaki, R., Watanabe, K., and Yamaguchi, Y. Overproduction of hyaluronan by expression of the hyaluronan synthase Has2 enhances anchorage-independent growth and tumorigenicity. Cancer Res., *59:* 1141-1145, 1999.

21. Itano, N., Sawai, T., Miyaishi, O., and Kimata, K. Relationship between hyaluronan production and metastatic potential of mouse mammary carcinoma cells. Cancer Res. *59:* 2499-2504, 1999.

22. Chen, C., and Okayama, H . High-efficiency transformation of mammalian cells by plasmid DNA. Mol. Cell Biol. *7:* 2745-2752, 1987.

23. Green, S. J., Tarone, G., and Underhill, C. B. Distribution of hyaluronate and hyaluronate receptors in the adult lung. J. Cell Sci. *90:* 145-56, 1988.

24. Falk, W., Goodwin, R. H. and Leonard, E. J. A 48-well micro chemotaxis assembly for rapid and accurate measurement of leukocyte migration. J. Immunol. Meth. *33:* 239-247, 1980.

25. Yang, B., Yang, B. L., Savani, R. C., and Turley, E. A. Identification of a common hyaluronan binding motif in the hyaluronan binding proteins RHAMM, CD44 and link protein. EMBO J., *13:* 286-96, 1994.

26. Main, N. Analysis of cell-growth- phase-related variation in hyaluronate synthase activity of isolated plasma-membrane fractions of cultured human skin fibroblasts. Biochem. J., *237:* 333-342, 1986.

27. Tomida, M., Koyama, H., and Ono, T. Induction of hyaluronic acid synthetase activity in rat fibroblasts by medium change of confluent cultures. J. Cell Physiol. *86:* 121-130, 1975.

28. Hronowski, L., and Anastassiades, T. P. The effect of cell density on net rates of glycosaminoglycan synthesis and secretion by cultured rat fibroblasts. J. Biol. Chem. *255:* 10091-10099, 1980.

29. Matuoka, K., Namba, M., and Mitsui, Y. Hyaluronate synthetase inhibition by normal and transformed human fibroblasts during growth reduction. J. Cell Biol., *104:* 1105-1115, 1987.

30. West, D. C., Hampson, I. N., Arnold, F., and Kumar, S. Angiogenesis induced by degradation products of hyaluronic acid. Science, *228:* 1324-1326, 1985.

31. West, D. C. and Kumar, S. The effect of hyaluronate and its oligosaccharides on endothelial cell proliferation and monolayer integrity. Exp. Cell Res., *183:* 179-196, 1989.

32. Underhill, C. B. and Toole, B. P. Transformation-dependent loss of the hyaluronate-containing coats of cultured cells. J. Cell. Physiol., *110:* 123-128, 1982.

33. Koshiishi, I., Shizari, M. and Underhill, C. B. CD44 mediates the adhesion of platelets to hyaluronan. Blood, *84:* 390-396, 1994.

34. Brecht, M., Mayer, U., Schlosser, E., and Prehm, P. Increased hyaluronate synthesis is required for fibroblast detachment and mitosis. Biochem. J., *239:* 445-450, 1986.

35. Lark, M. W., and Culp, L. A. Selective solubilization of hyaluronic acid from fibroblast substratum adhesive sites. J. Biol. Chem. *257:* 14073-14080, 1982.

36. Abatangelo, G., Cortivo, R., Martelli, M., and Vecchia, P. Cell detachment mediated by hyaluronic acid. Exp. Cell Res., *137:* 73-78, 1982.

37. Folkman, J. New perspectives in clinical oncology from angiogenesis research. Eur. J. Cancer; *32A:* 2534-2539, 1996.

38. Folkman, J. Angiogenesis and angiogenesis inhibition: an overview. EXS, *79:* 1-8, 1997.

39. Folkman, J., and D'Amore, P. A. Blood vessel formation: what is its molecular basis? Cell, *87:* 1153-1155, 1996.

40. Folkman ,J. Fighting cancer by attacking its blood supply. Sci. Am. *275:* 150-154, 1996.

41. Ohya, T., and Kaneko, Y. (1970) Novel hyaluronidase from Streptomyces hyalurolyticus. *Biochim. Biophys. Acta* **198**, 607-609.

42. Maniotis, A.J., Folberg, R., Hess, A., Sftor, E.A., Gardner, L.M., Pe'er, J., Trent, J.M., Meltzer, P.S., and Hendrix, M.J. (1999) Vascular channel formation by human melanoma cells in vivo and in vitro: vasculogenic mimicry. *Am. J. Pathol.* **155**, 739-752

Hyaluronan Synthase 3 Overexpression Promotes the Growth of TSU Prostate Cancer Cells[1]

Ningfei Liu, Feng Gao, Zeqiu Han, Xueming Xu, Charles B. Underhill, and Lurong Zhang[2]

Department of Oncology, Lombardi Cancer Center, Georgetown University Medical School, Washington DC 20007

ABSTRACT

Hyaluronan synthase 3 (HAS3) is responsible for the production of both secreted and cell-associated forms of hyaluronan and is the most active of the three isoforms of this enzyme in adults. In this study, the cDNA for human HAS3 was cloned and characterized. The open reading frame consisted of 1659 bp coding for 553 amino acids with a deduced molecular weight of about 63,000 and isoelectric pH of 8.70. The sequence of human HAS3 displayed a 53% identity to HAS1 and a 67% identity to HAS2. It also contained a signal peptide and six potential transmembrane domains, suggesting that it was associated with the plasma membrane. To evaluate the physiological role of human HAS3, expression vectors for this protein were transfected into TSU cells (a prostate cancer cell line), and the phenotypic changes in these cells were examined. The enhanced expression of hyaluronan in the transfected cells was demonstrated by dot blot analysis and ELISA. These cells were found to differ from their vector-transfected counterparts with respect to the following: (*a*) they grew at a faster rate in high (but not low) density cultures; (*b*) conditioned media from these cells stimulated the proliferation and migration of endothelial cells; (*c*) when placed on the chorioallantoic membrane of chicken embryos, these cells formed large, dispersed xenografts, whereas the control transfectants formed compact masses; and (*d*) when injected s.c. into nude mice, the xenografts formed by HAS3 transfectants were bigger than those formed by control transfectants. Histological examination of these xenografts revealed the presence of extracellular hyaluronan that could act as conduits for the diffusion of nutrients. In addition, they had a greater number of blood vessels. However, the HAS3-transfected TSU cells did not display increased metastatic properties as judged by their ability to form lung masses after i.v. injection. These results suggested that the HAS3-induced overexpression of hyaluronan enhanced tumor cell growth, extracellular matrix deposition, and angiogenesis but was not sufficient to induce metastatic behavior in TSU cells.

INTRODUCTION

A number of studies have suggested that the production of hyaluronan is associated with the metastatic behavior of tumor cells (1–11); e.g., Toole et al. (1) have shown that invasive tumors formed by V2 carcinoma cells in rabbits have higher concentrations of hyaluronan than noninvasive tumors formed by these same cells in nude mice. Similarly, Kimata et al. (2) found that a strain of mouse mammary carcinoma cells with a high metastatic potential produced significantly greater amounts of hyaluronan than a similar strain with a low metastatic potential. In a previous study (3), we found that the amount of hyaluronan on the surfaces of mouse B16 melanoma cells was directly correlated with their ability to form lung metastases. Finally, increased levels of hyaluronan production have been correlated with a variety of metastatic tumors, including carcinomas of the breast, lung,

liver, pancreas, and kidney (Wilms' tumor) (4–9). Indeed, in the case of Wilms' tumor (10) and mesotheliomas (11), the increased levels of hyaluronan in the serum of these patients has been regarded as a diagnostic marker for the clinical course of these conditions. Thus, there appears to be a correlation between hyaluronan production and metastatic behavior.

At present, three closely related isoforms for HAS[3] have been described, termed HAS1, 2, and 3, each of which appears to be associated with the plasma membrane (12–19). They have a predicted molecular mass of approximately 63 kDa, and transfection of cells with expression vectors for each of these isoforms can induce the synthesis of hyaluronan and the formation of a pericellular coat. However, the three isoforms are distinguished from each other with respect to: (*a*) their expression pattern during embryonic development and distribution in adult tissues; (*b*) the phenotype of knockout mutants in mice in which loss of HAS2 resulted in an embryonic lethality, whereas ones deficient in HAS1 and HAS3 were viable and had no obvious phenotype; (*c*) the rate at which they carry out hyaluronan synthesis, with HAS3 being more active than either HAS1 and HAS2; and (*d*) the size of the hyaluronan produced by the different isoforms with HAS3 giving rise to a somewhat smaller product than either HAS1 or 2 (17, 18).

Several recent studies have shown that transfection of tumor cells with expression vectors for hyaluronan synthase alters their behavior; e.g., Kosaki et al. (20) reported that the transfection of human fibrosarcoma cells with HAS2 enhanced both anchorage-independent growth and tumorigenicity. In addition, Itano et al. (21) have found that clones of mouse mammary cancer cells that had low levels of hyaluronan synthesis demonstrated decreased metastatic properties, which could be restored if the cells were transfected with an expression vector for HAS1.

In this study, we have cloned and characterized the full-length cDNA for human HAS3 and examined its potential role in tumor progression. An expression vector carrying HAS3 was transfected into TSU prostate cancer cells, and alterations in the phenotype of the resulting cells were examined. We found that the HAS3-induced overexpression of hyaluronan enhanced the rate of tumor cell growth both in vitro and in vivo. Xenografts of the HAS3-transfected cells grew faster and larger, demonstrated a hyaluronan-rich stroma and increased vascularization. However, transfection with HAS3 did not shift the TSU cells to a more metastatic phenotype, suggesting that hyaluronan alone is not sufficient for metastasis in the case of TSU cells.

MATERIALS AND METHODS

Cell Lines. The TSU human prostate cancer cell line was obtained from the Tumor Cell Line Bank of the Lombardi Cancer Center (Georgetown University, Washington DC) and maintained in 10% calf serum, 90% DMEM. ABAE cells were kindly provided by Dr. Luyuan Li (Lombardi Cancer Center, Washington DC) and were cultured in 10% fetal bovine serum, 90% DMEM containing 2 ng/ml basic fibroblast growth factor.

[3] The abbreviations used are: HAS, hyaluronan synthase; ABAE, adult bovine aorta endothelial cells; b-HABP, biotinylated hyaluronan-binding protein from cartilage; RT-PCR, reverse transcription-polymerase chain reaction.

Cloning and Characterization of cDNA for Human HAS3. Oligonucleotide primers for PCR of a partial sequence of cDNA for human HAS3 were designed according to the published sequence of Spicer and McDonald (Ref. 17; GenBank accession no. U86409) and consisted of the following: 5'-TCCTACTTTGGCTGTGTGCAG and 3'-AGATTTGTTGATGGTAGCAAT. A human brain cDNA library (Clontech, Palo Alto, CA) was used as a template, and PCR was performed to generate a 570-bp fragment of human HAS3 cDNA. This fragment was then used to probe the human brain cDNA library. Positive clones were isolated, amplified, and sequenced. The Mac-Vector program was used to carry out homologue analysis of the cloned human HAS3 with other human and mouse HASs.

Construction and Transfection of Human HAS3 Expression Vector. The cDNA for HAS3 was subcloned into the pcDNA3 mammalian expression vector (Invitrogen, Carlsbad, CA), and correct clones were identified by restriction endonuclease map analysis. The HAS3-pcDNA3 or pcDNA3 (control vector) were transfected into TSU cells using the calcium precipitation method (22). The clones that survived in 1 mg/ml of Geneticin (G418) (>100 individual clones in each case) were pooled and expanded for further characterization.

Characterization of Transfected Cells. The presence of HAS3 message was determined by RT-PCR using the GeneAmp RNA PCR kit (Perkin-Elmer, Branchburg, NJ). The primers consisted of the following: 5'-TCATGGTGGT-GGATGGCAACCGC and 3'-CTAAGCCACCTGATGTACGTCCA, which gave rise to a 283-bp reaction product with HAS3 and a 324-bp product with HAS1. The amplified sequences were analyzed by agarose gel electrophoresis followed by staining with ethidium bromide.

Two methods were used to determine hyaluronan production by the transfected cells. The first consisted of dot blot analysis of secreted hyaluronan, in which conditioned media from vector-TSU and HAS3-TSU cells that had been cultured at similar densities for 3 days were applied to nitrocellulose membrane using a dot blot apparatus. After washing with PBS containing 0.1% Tween 20, the membrane was blocked with 5% nonfat milk and 1% polyvinylpyrrolidone in PBS for 30 min. The hyaluronan was detected by sequential incubations in 1 μg/ml of b-HABP (23) for 1 h, 0.25 μg/ml of peroxidase-labeled streptavidin for 1 h, and finally a chemiluminescent substrate for peroxidase.

The second method for quantitation of hyaluronan consisted of a modified enzyme-linked assay (23). For this assay, a high-bound ELISA plate (Falcon, Lincoln Park, NJ) was coated with 100 μg/ml of crude human umbilical cord hyaluronan (Sigma Chemical Co., St. Louis, MO) in PBS at room temperature overnight and blocked with 10% calf serum, 90% PBS. The samples of conditioned media and cell lysates were adjusted to equal protein concentrations, and 25-μl samples were mixed with 100 μl of 50 μg/ml of b-HABP at 37°C for 1 h and then transferred to the hyaluronan-coated ELISA plate. The unbound b-HABP remaining in the sample mixture could then bind to the hyaluronan-coated plate and was detected by incubation with 0.5 μg/ml of peroxidase-labeled streptavidin followed by a peroxidase substrate consisting of H_2O_2 and azinobis (3-ethyl-benzthiazoline sulfonic acid) in 0.1 M Na citrate (pH 5.0). The plate was read at A^{405}, and the concentration of hyaluronan in the samples was calculated from a standard curve.

The expression of CD44 by the vector-TSU and HAS3-TSU cells was examined by Western blotting. For this, both low- and high-density cultures were harvested with EDTA in PBS, and equivalent amounts of protein were dissolved in Laemmli sample buffer under nonreducing conditions and electrophoresed on a 10% SDS polyacrylamide gel. The resulting gel was electrophoretically transferred to a sheet of nitrocellulose and stained for CD44 using the BU52 monoclonal antibody (The Binding Site, Birmingham, United Kingdom) as described previously (24).

Anchorage-dependent Growth. Aliquots of medium (10% calf serum, 90% DMEM) containing 5000 transfected cells were added to 24-well dishes. At various times, the cells were harvested in 5 mM EDTA in PBS, and the cell number was determined with a Coulter counter. In some experiments, the cells were grown in the presence of 2 to 200 μg/ml of high molecular weight hyaluronan (Lifecore Biomedical, Chaska, MN) for 7 days.

Colony Formation. Vector-TSU or HAS3-TSU cells (20,000) were suspended in 1 ml of 0.36% agarose, 10% fetal bovine serum, 90% DMEM and then immediately placed on top of a layer of 0.6% solid agarose with 10% fetal bovine serum, 90% DMEM. Two weeks later, the number of colonies larger

than 50 μm in diameter was quantified using an Omnicon Image Analysis system (Imaging Products International, Chantilly, VA).

Endothelial Cell Proliferation and Migration. For the proliferation assay, 2×10^3 ABAE cells were subcultured into 96-well plates and allowed to grow overnight. The next day, the media was replaced with 150 μl of 1% calf serum, 99% DMEM along with 50 μl of conditioned medium from either vector-TSU or HAS3-TSU cells. After 36 h, 0.3 μCi of [^{3}H]thymidine was added to each well, and 8 h later the cells were processed with an autoharvester. The incorporated [^{3}H]thymidine was determined with a β-counter.

For the migration assay, 25-μl aliquots of 10% FCS, 90% DMEM containing 5×10^3 ABAE cells were added to bottom wells of a 48-well Boyden chamber (Nucleopore, Pleasanton, CA) and then covered with a nucleopore membrane (5-μm pore size) coated with 0.1 mg/ml gelatin (25). The top well chamber was assembled and inverted for 2 h to allow the cells to adhere to the bottom side of membrane and then turned upright. Conditioned medium (50 μl) from either the vector-TSU or HAS3-TSU cells was added to top wells of the chamber and incubated for 2 h. The membrane was removed, the bottom side was carefully wiped to remove cells that had not migrated, and then the cells on the topside were stained with Hema 3 (Biochemical Science, Swedenboro, NJ). The membrane was placed on a slide, and the number of cells that had migrated to the topside were counted in 10 random high-powered fields.

Tumor Growth and Metastasis Assay. Two assay systems were used to determine tumor growth in vivo. In the first assay, 2×10^6 vector-TSU and

```
                           G TGC GTT CGC GGC TGC TTT GAC CTG GTG GGC GCC GCC TCC
GGC ACT GCA CCG AGG CGG GGC GGC GCC AGC GCC CAG GTT GCT GGG CTG GCC TTG GGC CCC CCT
TCC CCT ACC CAG AGC GCA GGC AGG CAG GGG GGT CCC GCC GCG CCC CTT CAG CAT ATG CCG160
                                                                     M   P   2
GTG CAG CTG ACG ACA GCC CTG CGT GTG GTG GGC ACC AGC CTG TTT GCC CTG GCA GTG CTG 220
 V   Q   L   T   T   A   L   R   V   V   G   T   S   L   F   A   L   A   V   L   22
GGT GGC ATC CTG GCA GCC TAT GTG ACG GGC TAC CAG TTC ATC CAC ACG GAA AAG CAC TAC 280
 G   G   I   L   A   A   Y   V   T   G   Y   Q   F   I   H   T   E   K   H   Y   42
CTG TCC TTC GGC CTG TAC GGC GCC ATC CTG GGC CTG CAC CTC CTC ATT CAG AGC CTT TTT 340
 L   S   F   G   L   Y   G   A   I   L   G   L   H   L   L   I   Q   S   L   F   62
GCC TTC CTG GAC CAC CGG CGC ATG CAA CGT GCC GGC CAG GCC CTG AAG CTG CCC TCC CCG 400
 A   F   L   D   H   R   R   M   Q   R   A   G   Q   A   L   K   L   P   S   P   82
CGG CGG GGC TCG GTG GCA CTG TGC ATT GCC GCA TAC CAG GAG GAC CCT GAC TAC TTG CGC 460
 R   R   G   S   V   A   L   C   I   A   A   Y   Q   E   D   P   D   Y   L   R   102
AAG TGC CTG CGC TCG GCC CAG CGC ATC TCC TTC CCT GAC CTC AAG GTG GTC ATG GTG 520
 K   C   L   R   S   A   Q   R   I   S   F   P   D   L   K   V   V   M   V   V   122
GAT GGC AAC CGC CAG GAG GAC GCC TAC ATG CTG GAC ATC TTC CAC GAG GTG CTG GGC GGC 580
 D   G   N   R   Q   E   D   A   Y   M   L   D   I   F   H   E   V   L   G   G   142
ACC GAG CAG GCC GGC TTC TTT GTG TGG CGC AGC AAC TTC CAT GAG GCA GGC GAG GGT GAG 640
 T   E   Q   A   G   F   F   V   W   R   S   N   F   H   E   A   G   E   G   E   162
ACG GAG GCC AGC CTG CAG GAG GGC ATG GAC CGT GTG CGG GAT GTG GTG CGG GCC AGC ACC 700
 T   E   A   S   L   Q   E   G   M   D   R   V   R   D   V   V   R   A   S   T   182
TTC TCG TGC ATC ATG CAG AAG TGG GGA GGC AAG CGC GAG GTC ATG TAC ACG GCC TTC AAG 760
 F   S   C   I   M   Q   K   W   G   G   K   R   E   V   M   Y   T   A   F   K   202
GCC CTC GGC GAT TCG GTG GAC TAC ATC CAC GTG TGC GAC TCT GAC ACT GTG CTG GAT CCA 820
 A   L   G   D   S   V   D   Y   I   Q   V   C   D   S   D   T   V   L   D   P   222
GCC TGC ACC ATC GAG ATG CTT CGA GTC CTG GAG GAG GAT CCC CAA GTA GGG GGA GTC GGG 880
 A   C   T   I   E   M   L   R   V   L   E   E   D   P   Q   V   G   G   V   G   242
GGA GAT GTC CAG ATC CTC AAC AAG TAC GAC TCA TGG ATT TCC TTC CTG GAC AGC GTG CGG 940
 G   D   V   Q   I   L   N   K   Y   D   S   W   I   S   F   L   S   S   V   R   262
TAC TGG ATG GCC TTC AAC GTG GAG CGG GCC TGC CAG TCC TAC TTT GGC TGT GTG CAG TGT1000
 Y   W   M   A   F   N   V   E   R   A   C   Q   S   Y   F   G   C   V   Q   C   282
ATT AGT GGG CCC TTG GGC ATG TAC CGC AAC AGC CTC CTG CAA CAG TTC CTG GAG GAC TGG1060
 I   S   G   P   L   G   M   Y   R   N   S   L   L   Q   Q   F   L   E   D   W   302
TAC CAT CAG AAG TTC CTA GGC AGC AAG TGC AGC TTC GGG GAT GAC CGC CTC ACC AAC1120
 Y   H   Q   K   F   L   G   S   K   C   S   F   G   D   D   R   H   L   T   N   322
CGA GTC CTG AGC CTT GGC TAC CGA ACT AAG TAT ACC GCC TCC AAG TAC CTC ACA GAG1180
 R   V   L   S   L   G   Y   R   T   K   Y   T   A   R   S   K   C   L   T   E   342
ACC CCC ACT AAG TAC CTC CGG CTC GTC AAC CAA ACC CGC TGG AGC AAG TCT TAC TTC1240
 T   P   T   K   Y   L   R   W   L   N   Q   Q   T   R   W   S   K   S   Y   F   362
CGG GAG TGG CTC TAC AAC TCT CTG TGG TTC CAT AAG CAC CAC CTC TGG ATG ACC TAC GAG1300
 R   E   W   L   Y   N   S   L   W   F   H   K   H   H   L   W   M   T   Y   E   382
TCA GTG GTC ACG GGT TTC TTC CCC TTC TTC CTC ATT GCC ACG GTT ATA CAG CTT TTC TAC1360
 S   V   V   T   G   F   F   P   F   F   L   I   A   T   V   I   Q   L   F   Y   402
CGG GGC CGC ATC TGG AAC ATT CTC CTC TTC CTG CTG ACG GTG CAG CTG GTG GGC ATT ATC1420
 R   G   R   I   W   N   I   L   L   F   L   L   T   V   Q   L   V   G   I   I   422
AAG GCC ACC TAC GCC TGC TTC CTT CGG GGC AAT GCA GAG ATG ATC TTC ATG TCC CTC TAC1480
 K   A   T   Y   A   C   F   L   R   G   N   A   E   M   I   F   M   S   L   Y   442
TCC CTC CTC TAT ATG TCC AGC CTT CTG CCG GCC AAG ATC TTT GCC ATT GCT ACC ATC AAC1540
 S   L   L   Y   M   S   S   L   L   P   A   K   I   F   A   I   A   T   I   N   462
AAA TCT GGC TGG GGC ACC TCT GGC CGA AAA ACC ATT GTG GTG AAC TTC ATT GGC CTC ATT1600
 K   S   G   W   G   T   S   G   R   K   T   I   V   V   N   F   I   G   L   I   482
CCT GTG TCC ATC TGG GTG GCA GTT CTC CTG GGA GGC CTG GCC TAC ACA GCT TAT TGC CAG1660
 P   V   S   I   W   V   A   V   L   L   G   G   L   A   Y   T   A   Y   C   Q   502
GAC CTG TTC AGT GAG ACA GCA GCG CTC GCC TTC CTT GTC TCT GGG GCT ATA CTG TAT GGC1720
 D   L   F   S   E   T   E   L   A   F   L   V   S   G   A   I   L   Y   G   C   522
TAC TGG GTG GCC CTC CTC ATG CTA TAT CTG GCC ATC ATC GCC CGA TGT GGG AAG AAG1780
 Y   W   V   A   L   L   M   L   Y   L   A   I   I   A   R   R   C   G   K   K   542
CCG GAG CAG TCA AGC TTG GCT TTT GCT GAG GTG TGA CAT GGC CCC CAA GCA GAG CGG GTA1840
 P   E   Q   S   S   L   A   F   A   E   V   *                                   553
AAG TGC AAT GGG TAA GGG AGG GAA GGG GAA TGG AAG AGA AAA GAC AGG GTG GGA GGG AGG1900
AGG GAG TGC TGT GTT TTA GTC TCT TAA TGG TCC AAA GGA CAA ATC TAA AAT GCA AAG AAC1960
GGT GAT GTA GTA TGG CCT GAC AGC TGT GTT TA                                     1992
```

Fig. 1. Nucleotide sequence and derived amino acid sequence of human HAS3. The open reading frame of human HAS3 consists of 1659 bp coding for 553 amino acids. The signal peptide (first 27 amino acids) and the six transmembrane domains are *underlined*. Between the first transmembrane domain (amino acids 43 to 65) and the second transmembrane domain (amino acids 384 to 402) there is a stretch of 319 amino acids located outside of the plasma membrane, which is probably the major functional region for the synthase activity. The remaining 170 amino acids in the COOH terminus (amino acids 384 to 553) contain five transmembrane domains that can form loops that span the plasma membrane. The GenBank accession no. is AF234839.
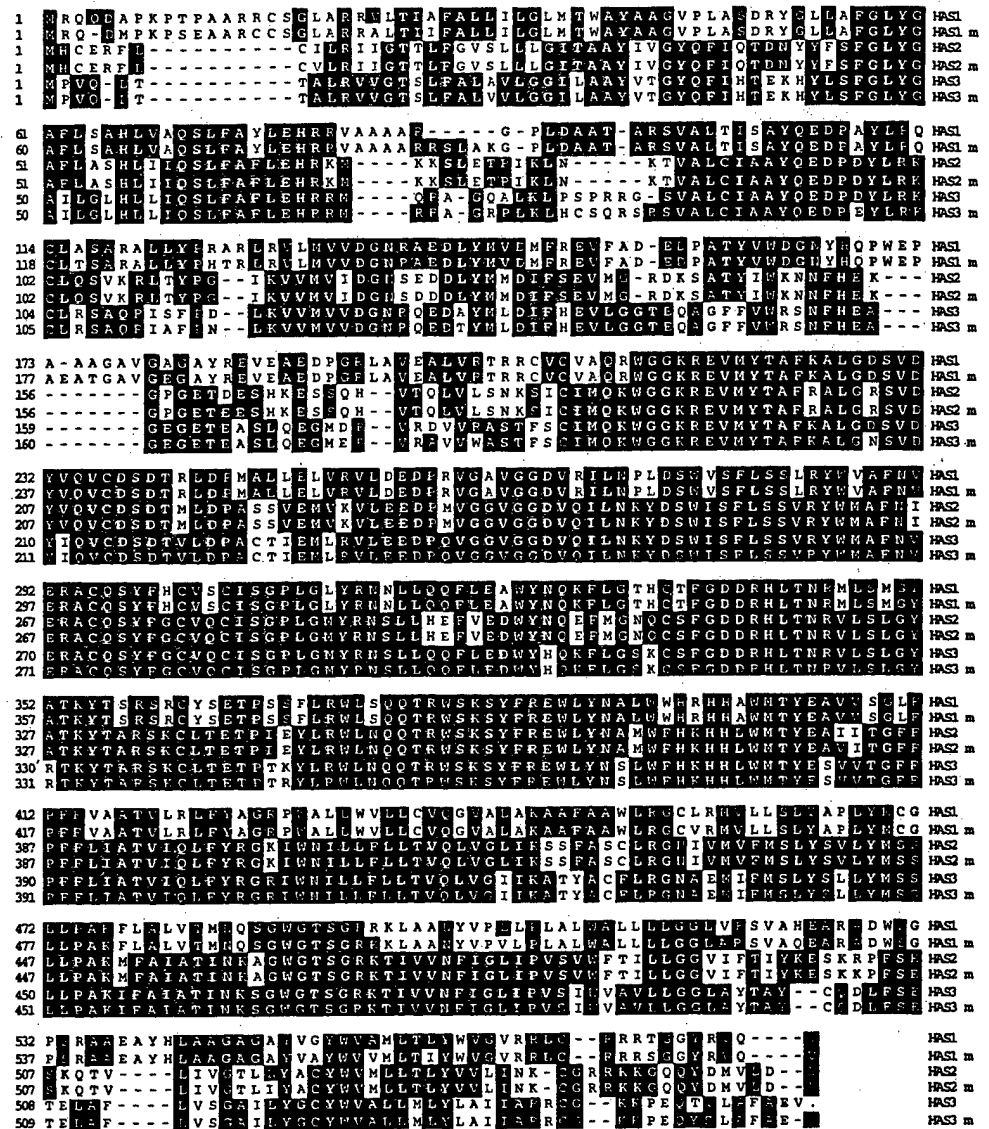
Fig. 2. Comparison of the human HAS3 with other members of the HAS family. Human HAS3 is about 53% identical to HAS1, 67% identical to HAS2 of both human and mouse (m), and 96% identical to mouse HAS3.

HAS3-TSU cells were placed on the chorioallantoic membranes of 10-day-old chicken embryos (15 eggs/group) and incubated at 37°C for 5 days. The tumor masses that grew on the chorioallantoic membranes were removed, photographed, and weighed. In the second assay system, the transfected cells were injected s.c. into 5-week-old male nude mice (2 × 10⁶ cells/site; five mice/group), and the size of the xenografts was measured twice a week. At the end of 3 weeks, the mice were sacrificed, and the xenografts were photographed, weighted, and then fixed with 3.7% formaldehyde or frozen in liquid nitrogen for immunohistochemical staining.

To examine experimental metastasis, 5 × 10⁵ vector-TSU and HAS3-TSU cells were injected into the tail veins of 5-week-old nude mice (five mice/group). Three weeks later, the mice were sacrificed, and the lungs were examined under a dissecting microscope for metastases.

Histological Staining. To stain cultured cells for hyaluronan, the transfected cells were seeded into an 8-well chamber slide (Nunc, Naperville, IL) and allowed to grow to confluence. After fixation in 3.7% formaldehyde for 5 min, the cells were washed and stained with 10 μg/ml b-HABP in 10% calf serum, 90% PBS, followed by 4 μg/ml of peroxidase-conjugated streptavidin and finally a substrate consisting of 3-amino-9-ethyl-carbazole and H₂O₂ that gives a dark red reaction product (23).

To stain xenografts for hyaluronan, the tissue was fixed with formaldehyde, embedded in paraffin, and cut into 5-μm thick sections. After the removal of the paraffin, the sections were processed as described above. After the immunoperoxidase reaction step, the sections were counter-stained with Mayer's hematoxylin and then preserved with Crystal/Mount (Biomeda, Foster City, CA).

To stain for endothelial cells, samples of the xenografts were rapidly frozen, cut into 10-μm thick sections, fixed in acetone, and air-dried. The sections were incubated sequentially with: (a) a 1:30 dilution of rat antimouse CD31 (PharMigen, San Diego, CA) in 10% calf serum, 90% PBS for 1 h; (b) avidin-biotin complex method reagents for rat IgG (ABC kits; Biomeda); (c) a peroxidase substrate consisting of H₂O₂ and 3-amino-9-ethyl-carbazole; and (d) counter-stained with Mayer's hematoxylin. The numbers of immunopositive spots corresponding to small blood vessels were counted in 10 random fields of three samples from each group.

Statistical Analysis. The mean and SE were calculated from the raw data and then subjected to Student's t test. The $P < 0.05$ was regarded as statistically significant.

RESULTS

Cloning and Characterization of Human HAS3. The full-length cDNA for HAS3 was cloned from a cDNA library of human brain using a probe consisting of a known partial sequence of the gene. The open reading frame contained 1659 bp coding for 553 amino acids and is shown in Fig. 1. The HAS3 protein had a deduced molecular weight of about 63,000 and a pI of 8.70. The first 27 amino acids represented
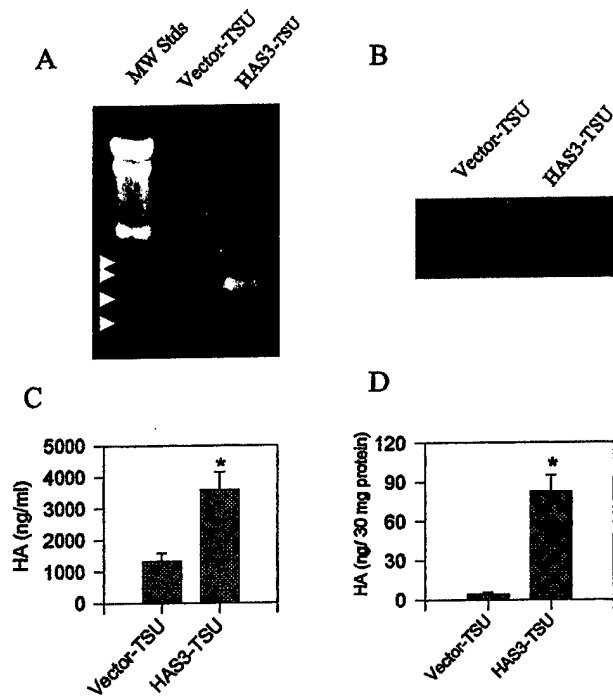
Fig. 3. Analysis of vector-TSU and HAS3-TSU cells for HAS3 mRNA and hyaluronan production. *A*, for the analysis of HAS3 message, RNA was extracted from the cultured cells and subjected to RT-PCR as described in "Materials and Methods." Agarose gel electrophoresis of the reaction products showed that the HAS3-TSU cells contained a prominent band of approximately 280 bp that was absent from the vector-TSU cells. The positions of markers for 100 through 400 bp are indicated by the *arrowheads* in the first *lane*. *B*, for the analysis of hyaluronan production, conditioned media from the transfected cells was applied to nitrocellulose using a dot blot apparatus and stained for hyaluronan using b-HABP, followed by peroxidase-labeled streptavidin and a chemiluminescence reagent. The dots represent the hyaluronan in conditioned media of vector-TSU cells (*left*) and HAS3-TSU cells (*right*). *C* and *D*, the amount of hyaluronan in conditioned media and cell lysates as determined by an ELISA are shown respectively. The increase of hyaluronan in conditioned media and lysates from HAS3-TSU cells as compared with the vector-TSU cells was statistically significant ($P < 0.05$).

the signal peptide (the cleavage site is between ILA and AY). There were six transmembrane sequences, one in the NH_2 terminus and five in the COOH terminus. Between the first transmembrane sequence (from amino acid 43 to 65) and second transmembrane sequence (from amino acid 384 to 402), there was a stretch of 319 amino acids located outside of plasma membrane, which appeared to be the major functional region for polysaccharide synthesis. The 170 amino acids in the COOH terminus (from amino acid 384 to 553) contained five transmembrane domains that can form loops spanning in and out of the plasma membrane. A potential N-glycosylation site was present at amino acid position 462, a glycosaminoglycan attachment site at position 464, and several phosphorylation sites for tyrosine kinase, casein kinase, protein kinase C, and cyclic AMP- and cyclic GMP-dependent protein kinases. HAS3 also contained seven hyaluronan-binding motifs of $B(X_7)B$ in which B is either R or K, and X_7 contains no acidic residues and at least one basic amino acid (26). Similar domains are present in other hyaluronan-binding proteins such as RHAMM, CD44, hyaluronidase, link protein, aggrecan, human GHAP, and TSG-6. Fig. 2 shows that compared with related enzymes, human HAS3 was about 53% identical to HAS1 (both human and mouse forms), 67% identical to HAS2, and 96% identical to mouse HAS3. These results are consistent with earlier studies of this and related genes (13–19).

Overexpression of Hyaluronan in TSU Cells Transfected with HAS3. To examine the role of HAS3 in tumor progression, the cloned cDNA was inserted into a mammalian expression vector (pcDNA3) under the control of a cytomegalovirus promoter and then

transfected into TSU cells (human prostate cancer). To avoid complications associated with clonal variations, all of the clones (>100) that survived in 1 mg/ml of Geneticin (G418) were pooled and expanded for experimental analysis throughout this study. The presence of HAS3 message in the transfected cells was examined by RT-PCR as described in "Materials and Methods." When analyzed by agarose gel electrophoresis (Fig. 3*A*), the HAS3-TSU cells gave rise to a PCR product of approximately 280 bp corresponding to HAS3, whereas no such band was detected in the vector-TSU cells. In addition, no reaction product of 314 bp was apparent, indicating that the message for HAS1 was absent from these cells.

The production of hyaluronan by the transfected cells was initially examined by dot blot analysis. As showed in Fig. 3*B*, conditioned medium from HAS3-TSU cells contained a significantly greater amount of hyaluronan than that from vector-TSU cells. To quantitatively measure the hyaluronan, a competitive enzyme-linked assay was performed. Fig. 3, *C* and *D* show that both conditioned medium and lysates of HAS3-TSU cells contained greater amounts of hyaluronan as compared with those of the control vector-TSU cells. However, there was no obvious difference in the level of CD44, a cell surface receptor for hyaluronan, on the two cell types at either low or high density as determined by Western blotting (data not shown). Taken together, these results indicate that the transfection of TSU cells with cDNA for HAS3 stimulated their production of hyaluronan.

HAS3 Promotes Cell Growth at High Densities. We then compared the growth rates of the vector-TSU and HAS3-TSU cells. For this, the transfected cells were subcultured at similar starting densities, and at various times thereafter the cells were harvested and enumerated with a Coulter counter. Fig. 4*A* shows that during the first 4 days, there was no obvious difference in the proliferation rates of the vector-TSU and HAS3-TSU cells. However, after day 5, the HAS3-TSU cells began to proliferate at a faster rate than the vector-TSU cells. Thus, at high densities, the HAS3-transfected cells grew at a faster rate. This conclusion was also suggested by our recent finding that transfection of MDA-231 human breast cancer cells with antisense to HAS3 results in decreased expression of hyaluronan and inhibition of their growth at high densities.[4] Together, these results indicate that HAS3 plays a role in cell proliferation at high densities.

Cultures of the vector-TSU and HAS3-TSU cells were then compared with respect to their patterns of growth and hyaluronan staining. As shown in Fig. 4*B* (*top*), the vector-TSU cells displayed a cobblestone appearance indicative of contact inhibition of growth with relatively little staining of pericellular hyaluronan. In contrast, the HAS3-TSU cells (Fig. 4*B*, *bottom*) appeared to have lost contact-inhibition of growth, forming numerous multilayered clusters of cells, which were associated with most of the hyaluronan staining. In addition, the HAS3-TSU cells displayed an enhanced ability to form colonies in soft agar as compared with the vector-TSU cells (Fig. 4*C*). Thus, at high densities, the HAS3-transfected cells grew at a faster rate, presumably because they had partially lost contact inhibition of growth.

Conditioned Medium from HAS3-TSU Stimulated the Proliferation and Migration of Endothelial Cells. Because several studies (27–29) reported that hyaluronan can modulate angiogenesis, we examined the effects of conditioned medium from HAS3-TSU cells on the behavior of cultured endothelial cells. When conditioned medium from HAS3-TSU cells was added to the medium of ABAE cells, it stimulated their proliferation by 66% as compared with that from vector-TSU cells (Fig. 5*A*). Furthermore, conditioned medium from the HAS3-TSU also stimulated the migration of ABAE cells through
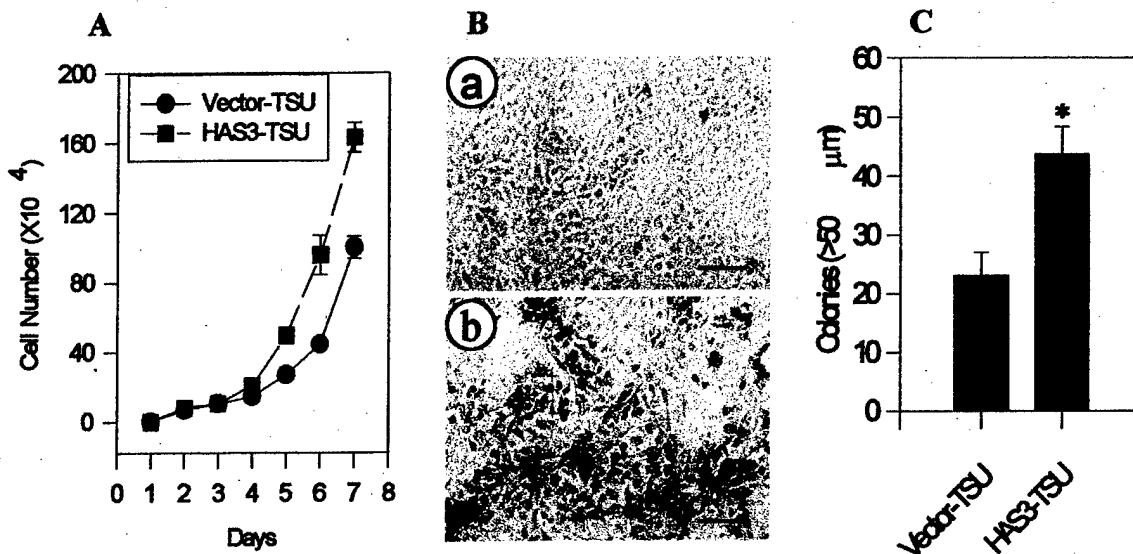
---

[4] Unpublished data.

Fig. 4. *In vitro* growth pattern of vector-TSU and HAS3-TSU cells. *A*, cell growth curves for the transfected TSU cells are shown. The cells were plated in 24-well dishes, and the cell number was determined at the indicated times. Although the rate of cell growth was the same at low densities, at higher densities, the HAS3-TSU cells grew faster than the vector-TSU cells. Three independent experiments yielded similar results. *B*, transfected cells at high density were stained for hyaluronan. The transfected cells were grown to confluence, briefly fixed in formaldehyde, and stained for hyaluronan with b-HABP, followed by peroxidase-labeled streptavidin and finally a substrate for peroxidase that gives a red color. The vector-TSU cells (*part a*) formed a confluent monolayer with little hyaluronan staining, whereas the HAS3-TSU cells (*part b*) formed numerous multilayered clusters that stain for hyaluronan (*bar*, 100 μm). *C*, anchorage-independent growth of the transfected cells is shown. Equal numbers of vector-TSU and HAS3-TSU cells were cultured in soft agar for 2 weeks, and the number of colonies were counted with Omnicon Image Analysis system. The HAS3-TSU cells formed a greater number of colonies larger than 50 μm than did the vector-TSU cells (*, $P < 0.05$). This experiment was performed in triplicate.

nucleopore filters by more than 300% as compared with conditioned medium from control cells (Fig. 5*B*). These results further suggest that the hyaluronan produced by HAS3-TSU cells could exert a stimulatory effect on endothelial cells.

The Growth of Transfected Cells on the Chicken Chorioallantoic Membrane. To determine whether the increased growth rate of HAS3-TSU cells *in vitro* also occurred *in vivo*, we examined their growth on the chorioallantoic membranes of chicken eggs. In this experiment, equal numbers of vector-TSU and HAS3-TSU cells were placed on the chorioallantoic membranes of 10-day-old chicken embryos and allowed to grow for 5 days. The xenografts showed a striking divergence in morphology. The vector-TSU cells formed rounded, nodular xenografts that grew out of the membrane surface, with necrotic tissue in the center, whereas the HAS3-TSU cells gave rise to xenografts with a dispersed morphology within the membrane and without any obvious signs of necrosis. As shown in Fig. 6, *A* and *B*, the HAS3-TSU xenografts were significantly larger than those of the vector-TSU cells. Histological examination of the xenografts revealed that, whereas the vector-TSU cells were compact, the HAS3-TSU cells were more dispersed with increased intercellular spaces (data not shown). These results suggested that overexpression of hyaluronan enhanced the tumor growth on the chorioallantoic membrane system.

HAS3 Promotes the Primary Growth of TSU Cells but Not Metastasis in Nude Mice. The *in vivo* growth characteristics of these cells were further examined by injecting them s.c. into nude mice. After 2 weeks, the xenografts formed by HAS3-TSU cells grew at a faster rate and appeared to be more vascularized than the control cells. After 3 weeks of growth, the HAS-3 xenografts were three times larger than those formed by the vector-TSU cells (Fig. 7, *A* and *B*), suggesting that HAS3 promotes the growth of TSU tumor cells in mice. These results are consistent with those obtained from the chicken chorioallantoic membrane system.

However, when transfected cells were injected into the tail veins of nude mice (five mice/group), no lung metastases were detected with

either cell type. Thus, the overexpression of hyaluronan by itself is not sufficient to induce metastatic behavior in TSU cells.

Increased Extracellular Hyaluronan and Angiogenesis in HAS3-TSU Xenografts. The xenografts from nude mice were processed for histology, and the resulting sections were stained for hyaluronan (Fig. 8*A*). Although the xenografts varied from region to region, in general, the cells in the vector-TSU xenografts were relatively homogeneous and compact, and most of the hyaluronan appeared to be present in the cytoplasm of the cells (Fig. 8*A*). In contrast, the HAS3-TSU cells formed small clusters or nests of cells that were
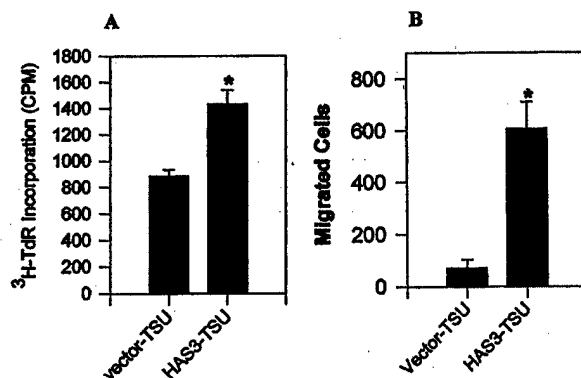

Fig. 5. Effect of conditioned media from vector-TSU and HAS3-TSU cells on endothelial cells. *A*, effects of conditioned media on the proliferation of endothelial cell are demonstrated. ABAE cells were cultured for 36 h in the presence of conditioned media from either vector-TSU or HAS3-TSU cells, pulsed with [^{3}H]thymidine for 8 h, harvested, and processed for incorporated radioactivity. The conditioned media from HAS3-TSU cells stimulated the ABAE cells to a greater extent than that from vector-TSU cells. *B*, effects of conditioned medium on the migration of endothelial cells is shown. Aliquots containing 5×10^3 ABAE cells were added to bottom wells of a 48-well Boyden chamber, covered with a nucleopore membrane, and then treated with 50 μl of conditioned medium for 2 h. The membrane was stained with Hema 3 and placed on a slide, and the migrated cells were counted in 10 random fields. Conditioned medium from HAS3-TSU cells significantly increased the migration of the endothelial cells as compared with that from the vector-TSU cells ($P < 0.05$).
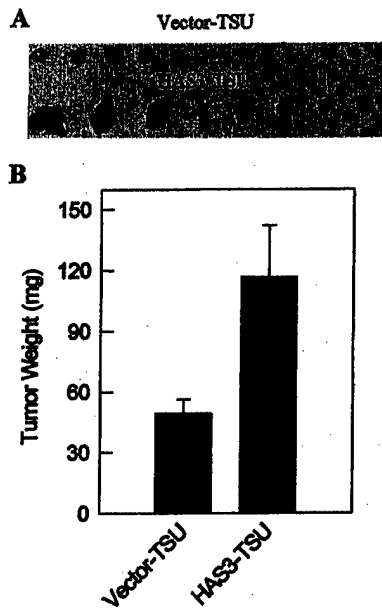
A

Vector-TSU

B

Fig. 6. Growth of transfected TSU cells on the chicken chorioallantoic membrane. Samples of vector-TSU and HAS3-TSU cells (2 × 10⁶ cells) were placed on the chorioallantoic membranes of 10-day-old chicken embryos (15 eggs/group), incubated at 37°C for 5 days, and then photographed. A, the xenografts of vector-TSU cells (top row) and HAS3-TSU cells (bottom row) from the chorioallantoic membrane are shown. The vector-TSU xenografts formed compact nodules, whereas the HAS3-TSU xenografts were more spread out and larger. B, the weights of the HAS3-TSU xenografts were significantly greater than that of the vector-TSU cells ($P < 0.05$).

surrounded by a matrix rich in hyaluronan (Fig. 8A). Such structures were not observed in the control-TSU xenografts.

The extent of angiogenesis in these xenografts was examined by staining for mouse endothelial cells using antibodies to CD31. Fig. 8B shows that there was strong positive staining in HAS3-TSU xenografts as compared with the control vector-TSU xenografts. The number of vessels in 10–15 random fields was significantly higher in the HAS3-TSU xenografts than in the control xenografts (Fig. 8C). This suggests that increased levels of hyaluronan can stimulate angiogenesis in mice, and this may, in part, account for the faster growth rate of tumors formed by HAS3-TSU cells.

DISCUSSION

In this study, we have characterized human HAS3 with regard to both its structure and its function in tumor progression. On the basis of its deduced amino acid sequence, HAS3 shares significant homology with HAS1 and HAS2, containing a signal peptide as well as six transmembrane regions strongly suggesting that it is associated with the plasma membrane. Its enzymatic activity was demonstrated by the fact that TSU cells transfected with expression vectors for HAS3 produced larger amounts of hyaluronan as determined by histochemical staining, dot blot analysis, and quantitative ELISA. These findings are consistent with earlier studies of HAS proteins (12–19).

This study also suggested that stimulation of hyaluronan synthesis in TSU cells by transfecting them with HAS3 expression vectors enhanced their growth both in chicken embryos and in nude mice. This enhanced tumor growth appeared to be attributable to two distinct mechanisms. The first involved a direct effect on the tumor cells themselves, as indicated by the fact that in tissue culture, HAS3-transfected cells grew at a faster rate at high density. The second mechanism promoting tumor growth rate resulted from an increase in vascularization, as reflected by the greater density of blood vessels in xenografts from nude mice. Together, these two factors contribute to the increased tumor growth rate.

At present, we believe that the effects of HAS3 transfection on TSU cell phenotype are a direct consequence of increased hyaluronan synthesis. Along these lines, it is important to note that HAS3 over-expression increases the production of both secreted and cell-associated hyaluronan. These two pools of hyaluronan may have different effects on cell behavior. This was suggested by preliminary experiments in which we found that the addition of high molecular weight hyaluronan to cultures of vector-TSU or HAS3-TSU cells had no obvious effect on their growth rates (data not shown). We believe that under these specific conditions, free hyaluronan of high molecular weight did not affect the behavior of these cells. Rather, we believe that it was the cell-associated fraction of hyaluronan induced by HAS3 that played a more important role in stimulating cell growth. However, we cannot eliminate the possibility that hyaluronan of the appropriate size and concentration may indeed influence the behavior of TSU cells, similar to the effects that it has on endothelial cells (27, 28). It is also possible that HAS3 may have effects on the TSU cells independent of its function to promote hyaluronan synthesis; e.g., HAS3 could influence the interaction of the plasma membrane with elements of the cytoskeleton and thereby alter cell behavior.

The hyaluronan on the surface of cultured cells can form a pericellular coat that can be directly visualized by its ability to exclude small particles such as erythrocytes (30). In the case of rat fibrosarcoma cells, this coat is composed of small, microvilli-like projections that extend out from the surface of the cells to which the hyaluronan is attached (31). This pericellular coat could stimulate the growth of cells by several different mechanisms. One possible mechanism is that it disrupts intercellular junctions and thereby allows the cells to detach from the substrate so that they can divide and occupy new space (32–34). This would allow cells to overcome contact inhibition of growth that is characteristic of TSU cells and allow them to from multilayers at high-density cultures as we have observed. Another possibility is that the hyaluronan interacts with receptors on the surfaces of cells such as CD44 or RHAMM to influence their migratory and proliferative behavior (35, 36).

Extracellular hyaluronan can also stimulate cell proliferation by
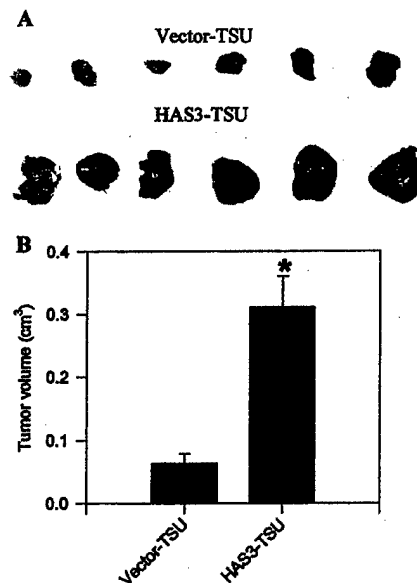
A

Vector-TSU

HAS3-TSU

B

Fig. 7. Xenografts formed by transfected TSU cells in nude mice. A, the appearance of xenografts formed in nude mice is shown. Mice received injections of 2 × 10⁶ vector-TSU cells (top) or HAS3-TSU cells (bottom), and the xenografts were harvested 21 days later. The HAS3-TSU xenografts were larger than those of the vector-TSU cells. B, the weights of the HAS3-TSU xenografts were significantly greater than that of the vector-TSU ($P < 0.05$).
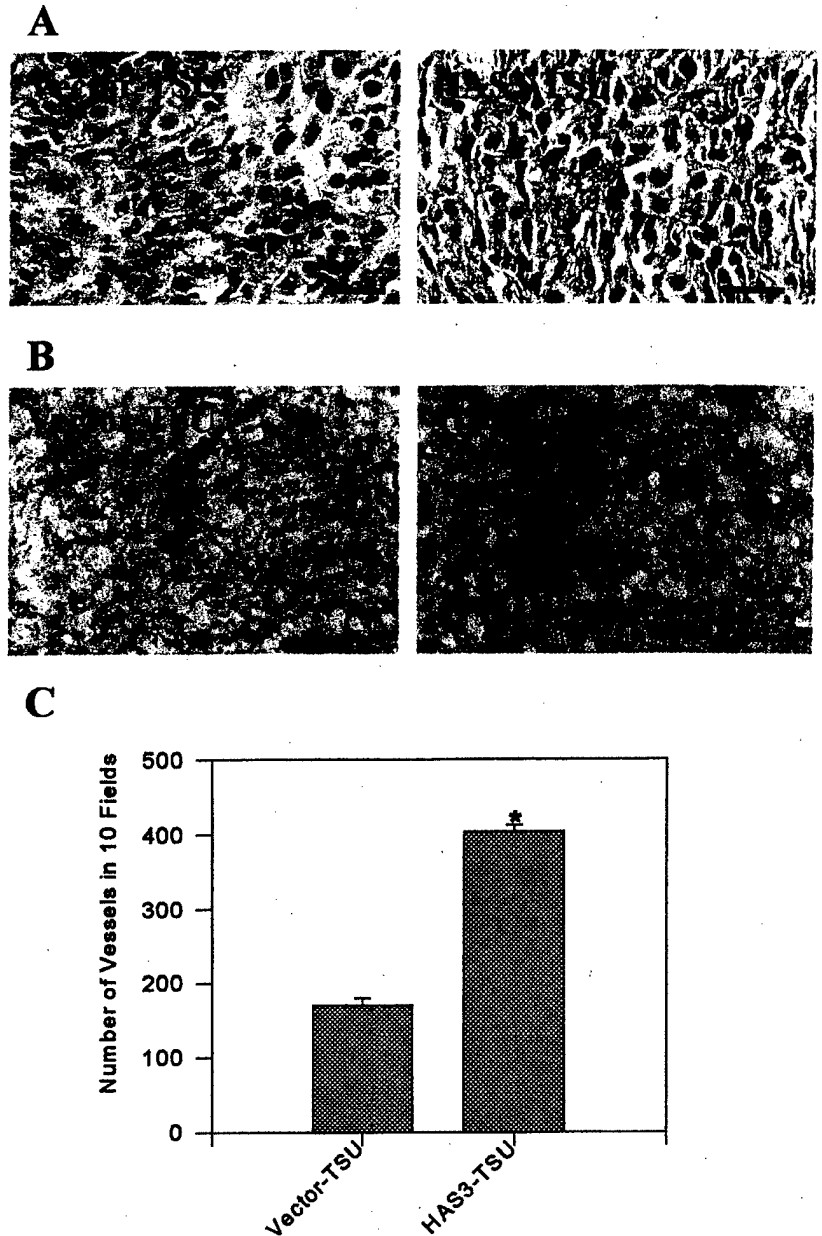
A

B

C

Fig. 8. Staining of xenografts for hyaluronan and endothelial cells. *A*, paraffin sections of vector-TSU and HAS3-TSU xenografts from nude mice were stained for hyaluronan (*red*) and counter-stained with hematoxylin (*blue*). A representative section of a vector-TSU xenograft shows that most of the hyaluronan staining was associated with the cytoplasm of the cells, whereas in a similar section from a HAS3-TSU xenograft, the cells were present in small clusters, surrounded by a stroma rich in hyaluronan. Although the microscopic morphology of the xenografts varied from region to region, the hyaluronan-rich stroma was prevalent in the HAS3-TSU xenografts and absent from the vector-TSU xenografts. *Bar*, 50 μm. *B*, cryostat sections of the xenografts were stained for endothelial cells using an antibody against mouse CD31. Representative fields show that xenografts formed from HAS3-TSU cells have a higher concentration of endothelial cells than those from vector-TSU cells. *Bar*, 100 μm. *C*, the number of blood vessels in 10 random fields from three samples of each group are shown. The HAS3-TSU xenografts had a significantly higher concentration of blood vessels than that of the vector-TSU cells ($P < 0.05$).

increasing the flow of nutrients. Indeed, the extracellular hyaluronan apparent in xenografts of HAS3-TSU cells in nude mice could serve as conduits through which nutrients diffuse to support cells located some distance from the blood supply and thus facilitate their growth. In the xenografts of vector-TSU cells that lacked these hyaluronan rich spaces, the tumor cells formed a continuous mass and were more susceptible to necrosis. Along these lines, extracellular hyaluronan is prominent in the lower regions of most, if not all, stratified epithelium, where it is believed to maintain spaces so that nutrients can diffuse to the more superficial epithelial cells (37, 38).

Hyaluronan also appeared to promote vascularization that is clearly important in regulating tumor growth (39, 40). This was indicated by our observation that xenografts of HAS3-TSU cells formed in nude mice had a greater density of blood vessels than did control xenografts. Part of this increased vascularization may be attributable to the pericellular spaces generated by the hyaluronan that provides space that facilitates the invasion of endothelial cells. In addition, the hyaluronan itself can stimulate the migration of endothelial cells. This was also indirectly suggested by experiments showing that condi-

tioned media from the HAS3-transfected cells stimulated the growth and migration of cultured endothelial cells. This is consistent with the earlier studies of West *et al.* (27, 28) who have shown that oligosaccharide fragments of hyaluronan stimulated the formation of new blood vessels in the chorioallantoic membrane of chicken embryos.

Although the results of this study suggest that overexpression of HAS3 in TSU prostate cancer cells promotes their tumorigenicity, there are some aspects that appear to contradict the findings of other studies; *e.g.*, although we found that TSU transfectants grew faster in culture, Kosaki *et al.* (20) found no such increase in the growth of HT1080 cells transfected with HAS2 under anchorage-dependent conditions; however, these cells did form larger colonies in suspension culture. We believe that this difference may be attributable in part to the different target cells that were used in these studies. The TSU cells used as targets in this study are of epithelial origin, whereas HT1080 cells are derived from a fibrosarcoma of connective tissue cells. This could also account for the differences seen with regard to growth behavior and the production of hyaluronan in the connective tissue and their ability to stimulate angiogenesis. Alternatively, the

differences could be attributed to the characteristics of the particular HASs that were used in these studies, because they differ with respect to both their synthetic activity as well as the size of the hyaluronan that they produce (16–18).

Another apparent discrepancy was our observation that transfection of TSU cells with HAS3 did not appear to stimulate their ability to form lung metastases in nude mice. In contrast, we had reported previously (3) that the levels of hyaluronan on the surface of B16 cells were directly correlated with their metastatic behavior. Similarly, Itano et al. (21) found that transfection of FM3A with HAS1 enhanced their metastatic properties. Again, we believe that these divergent results were attributable to the different cell types that were used as targets for transfection. In the case of B16 and FM3A, these cell lines originally possessed the ability to undergo metastasis, and stimulation of hyaluronan synthesis in these cells enhanced this innate property. In contrast, TSU cells appeared to lack this ability (at least in nude mice), and increased hyaluronan synthesis, by itself, is not sufficient to promote metastatic properties. Clearly, the process of metastasis is a complex phenomenon involving the collaboration of many molecules. Although the production of hyaluronan is one of the factors, it is not sufficient for tumor metastasis in the case of TSU cells.

In conclusion, the results of this study indicate that HAS3 expression plays a role in tumor progression and are consistent with earlier studies demonstrating a correlation between hyaluronan levels and tumorigenicity. Furthermore, the hyaluronan may be acting through several different mechanisms, including: (a) a direct effect on the growth of the tumor cells themselves; (b) the formation of extracellular conduits through which nutrients can flow; and (c) the stimulation of blood vessel growth. However, these effects depend upon the particular cell type and the specific environment. Given the complexity of the effects of hyaluronan, it may be difficult to predict exactly how it will influence the behavior of tumor cells. In the case of TSU cells, hyaluronan may be more of a facilitator of tumor growth rather than an instigator of metastasis.

REFERENCES

1. Toole, B. P., Biswas, C., and Gross, J. Hyaluronate and invasiveness of the rabbit V2 carcinoma. Proc. Natl. Acad. Sci. USA, 76: 6299–6303, 1979.
2. Kimata, K., Honma, Y., Okayama, M., Oguri, K., Hozumi, M., and Suzuki, S. Increased synthesis of hyaluronic acid by mouse mammary carcinoma cell variants with high metastatic potential. Cancer Res., 43: 1347–1354, 1983.
3. Zhang, L., Underhill, C. B., and Chen, L. Hyaluronan on the surface of tumor cells is correlated with metastatic behavior. Cancer Res., 55: 428–433, 1995.
4. Marotta, M., D'Armiento, F. P., Martino, G., Donato, G., Nazzaro, A., Vecchione, R., and Rosati, P. Glycosaminoglycans in human breast cancer: morphological and biochemical study. Appl. Pathol., 3: 164–169, 1985.
5. Coppes, M. J. Serum biological markers and paraneoplastic syndromes in Wilm's tumor. Med. Pediatr. Oncol., 21: 213–221, 1993.
6. Horai, T., Nakamura, N., Tateshi, R., and Hattori, S. Glycosaminoglycans in human lung cancer. Cancer (Phila.), 48: 2016–2021, 1981.
7. Roboz, J., Greaves, J., Silides, D., Chahinian, A. P., and Holland, J. F. Hyaluronic acid content of effusions as a diagnostic aid for malignant mesothelioma. Cancer Res., 45: 1850–1854, 1985.
8. Kojima, J., Nakamura, N., Kanatani, M., and Omori, K. The glycosaminoglycans in human hepatic cancer. Cancer Res., 35: 542–547, 1975.
9. Azumi, N., Underhill, C. B., Kagan, E., and Sheibani, K. A novel biotinylated probe specific for hyaluronate: its diagnostic value in diffuse malignant mesothelioma. Am. J. Surg. Pathol., 16: 116–121, 1992.
10. Dahl, I. M. S., and Laurent, T. C. Concentration of hyaluronan in serum of untreated cancer patients reference to patients with mesothelioma. Cancer (Phila.), 62: 326–330, 1988.
11. Frebourg, T., Lerebours, G., Delpech, B., Benhamou, D., Bertrand, P., Maingonnat, C., Boutin, C., and Nouvet, G. Serum hyaluronate in malignant pleural mesothelioma. Cancer (Phila.), 59: 2104–2107, 1987.
12. Shyjan, A. M., Heldin, P., Butcher, E. C., Yoshino, T., and Briskin, M. J. Functional cloning of the cDNA for a human hyaluronan synthase. J. Biol. Chem., 271: 23395–23399, 1996.
13. Watanabe, K., and Yamaguchi, Y. Molecular identification of a putative human hyaluronan synthase. J. Biol. Chem., 271: 22945–22948, 1996.
14. Itano, N., and Kimata, K. Molecular cloning of human hyaluronan synthase. Biochem. Biophys. Res. Commun., 222: 816–820, 1996.
15. Itano, N., and Kimata, K. Expression cloning and molecular characterization of HAS protein, a eukaryotic hyaluronan synthase. J. Biol. Chem., 271: 9875–9878, 1996.
16. Spicer, A. P., Olson, J. S., and McDonald, J. A. Molecular cloning and characterization of a cDNA encoding the third putative mammalian hyaluronan synthase. J. Biol. Chem., 272: 8957–8961, 1997.
17. Spicer, A. P., and McDonald, J. A. Characterization and molecular evolution of a vertebrate hyaluronan synthase gene family. J. Biol. Chem., 273: 1923–1932, 1998.
18. Spicer, A. P., and Nguyen, T. K. Mammalian hyaluronan synthases: investigation of functional relationships in vivo. Biochem. Soc. Trans., 27: 109–115, 1999.
19. Itano, N., Sawai, T., Yoshida, M., Lenas, P., Yamada, Y., Imagawa, M., Shinomura, T., Hamaguchi, M., Yoshida, Y., Ohnuki, Y., Miyauchi, S., Spicer, A. P., McDonald, J. A., and Kimata, K. Three isoforms of mammalian hyaluronan synthases have distinct enzymatic properties. J. Biol. Chem., 274: 25085–25092, 1999.
20. Kosaki, R., Watanabe, K., and Yamaguchi, Y. Overproduction of hyaluronan by expression of the hyaluronan synthase Has2 enhances anchorage-independent growth and tumorigenicity. Cancer Res., 59: 1141–1145, 1999.
21. Itano, N., Sawai, T., Miyaishi, O., and Kimata, K. Relationship between hyaluronan production and metastatic potential of mouse mammary carcinoma cells. Cancer Res., 59: 2499–2504, 1999.
22. Chen, C., and Okayama, H. High-efficiency transformation of mammalian cells by plasmid DNA. Mol. Cell. Biol., 7: 2745–2752, 1987.
23. Underhill, C. B., and Zhang, L. Analysis of hyaluronan using biotinylated hyaluronan-binding proteins. Methods Mol. Biol., 137: 441–447, 1999.
24. Culty, M., Shizari, M., Nguyen, H. A., Clarke, R., Thompson, E. W., and Underhill, C. B. Degradation of hyaluronan and expression of CD44 by human breast cancer cell lines correlate with their invasive potential. J. Cell. Physiol., 160: 275–286, 1994.
25. Falk, W., Goodwin, R. H., and Leonard, E. J. A 48-well micro chemotaxis assembly for rapid and accurate measurement of leukocyte migration. J. Immunol. Methods, 33: 239–247, 1980.
26. Yang, B., Yang, B. L., Savani, R. C., and Turley, E. A. Identification of a common hyaluronan binding motif in the hyaluronan binding proteins RHAMM, CD44 and link protein. EMBO J., 13: 286–296, 1994.
27. West, D. C., Hampson, I. N., Arnold, F., and Kumar, S. Angiogenesis induced by degradation products of hyaluronic acid. Science (Wash. DC), 228: 1324–1326, 1985.
28. West, D. C., and Kumar, S. The effect of hyaluronate and its oligosaccharides on endothelial cell proliferation and monolayer integrity. Exp. Cell Res., 183: 179–196, 1989.
29. Feinberg, R. N., and D. C. Beebe. Hyaluronate in vasculogenesis. Science (Wash. DC), 220: 1177–1179, 1983.
30. Underhill, C. B., and Toole, B. P. Transformation-dependent loss of the hyaluronate-containing coats of cultured cells. J. Cell. Physiol., 110: 123–128, 1982.
31. Koshiishi, I., Shizari, M., and Underhill, C. B. CD44 mediates the adhesion of platelets to hyaluronan. Blood, 84: 390–396, 1994.
32. Brecht, M., Mayer, U., Schlosser, E., and Prehm, P. Increased hyaluronate synthesis is required for fibroblast detachment and mitosis. Biochem. J., 239: 445–450, 1986.
33. Lark, M. W., and Culp, L. A. Selective solubilization of hyaluronic acid from fibroblast substratum adhesive sites. J. Biol. Chem., 257: 14073–14080, 1982.
34. Abatangelo, G., Cortivo, R., Martelli, M., and Vecchia, P. Cell detachment mediated by hyaluronic acid. Exp. Cell Res., 137: 73–78, 1982.
35. Zhang, S., Chang, M. C., Zylka, D., Turley, S., Harrison, R., and Turley, E. A. The hyaluronan receptor RHAMM regulates extracellular-regulated kinase. J. Biol. Chem., 273: 11342–11348, 1998.
36. Bourguignon, L. Y., Shu, H., Shao, L., and Chen, Y. W. CD44 interaction with Tiam1 promotes Rac1 signaling and hyaluronic acid-mediated breast tumor migration. J. Biol. Chem., 275: 1829–1338, 2000.
37. Alho, A. M., and Underhill, C. B. The hyaluronate receptor is preferentially expressed on proliferating epithelial cells. J. Cell Biol., 108: 1557–1565, 1989.
38. Underhill, C. B. The interaction of hyaluronate with the cell surface: the hyaluronate receptor and the core protein. Ciba Found. Symp., 143: 87–106, 1989.
39. Folkman, J. New perspectives in clinical oncology from angiogenesis research. Eur. J. Cancer, 32: 2534–2539, 1996.
40. Folkman, J., and D'Amore, P. A. Blood vessel formation: what is its molecular basis? Cell, 87: 1153–1155, 1996.